Identification by HPLC-ESI/MS of the Phosphorylated Peptides and Sites of Wheat Translation Initiation Factor (eIF) 4B *in Vitro*

by

Zhengming Shen

A dissertation submitted to the Graduate Faculty in Chemistry in partial fulfillment of the requirement for the degree of Doctor of Philosophy, The City university of New York

2004

Reproduced with permission of the copyright owner. Further reproduction prohibited without permission.

UMI Number: 3144139

Copyright 2004 by
Shen, Zhengming

All rights reserved.

INFORMATION TO USERS

The quality of this reproduction is dependent upon the quality of the copy submitted. Broken or indistinct print, colored or poor quality illustrations and photographs, print bleed-through, substandard margins, and improper alignment can adversely affect reproduction.

In the unlikely event that the author did not send a complete manuscript and there are missing pages, these will be noted. Also, if unauthorized copyright material had to be removed, a note will indicate the deletion.

UMI®

UMI Microform 3144139
Copyright 2004 by ProQuest Information and Learning Company.
All rights reserved. This microform edition is protected against unauthorized copying under Title 17, United States Code.

ProQuest Information and Learning Company
300 North Zeeb Road
P.O. Box 1346
Ann Arbor, MI 48106-1346

Reproduced with permission of the copyright owner. Further reproduction prohibited without permission.

Copyright

© 2004 (year degree awarded)

Zhengming Shen

All Rights Reserved. No part of this dissertation may be reproduced in any form or by any means, or stored in a database or retrieval system without permission in writing from the publisher.

Reproduced with permission of the copyright owner. Further reproduction prohibited without permission.

Approval Page

This manuscript has been read and accepted for the Graduate Faculty in

in satisfaction of the dissertation requirement for the degree of

Doctor of philosophy.

9/13/04
Date

Chair of Examining Committee

9/14/04
Date

Executive Officer

Peter N. Lipke

Gary J. Quigley

Supervisory Committee

THE CITY UNVERSITY OF NEW YORK

Reproduced with permission of the copyright owner. Further reproduction prohibited without permission.

ABSTRACT

Identification by HPLC-ESI/MS of the Phosphorylated Peptides and Sites of Wheat Translation Initiation Factor (eIF) 4B ***in Vitro***

by

Zhengming Shen

Mentor: Professor Dixie J. Goss

In wheat, the translation initiation factor eIF4B is a phosphoprotein whose phosphorylation state is developmentally regulated. To understand its biological role, the sites of phosphorylation have to be determined. Recombinant eIF4B protein expressed in *E. coli* was purified and subsequently phosphorylated by Casein Kinase II. Generally only limited amounts of proteins are phosphorylated. Here, we report a powerful technique for isolation of phosphorylated peptides with immobilized metal affinity chromatography (Fe(III)-IMAC) and direct High Pressure Liquid Chromatography/Electrospray Ionization Mass Spectrometry (HPLC-ESI/MS) analysis of phosphorylated peptides without any additional desalting steps.

For a purified protein digested with trypsin where each peptide sequence is known in a database, the phosphorylated peptide is confirmed in mass spectroscopic analysis by an increase of 80 Da (HPO_3) for each phosphorylated amino acid present compared with the calculated masses of the corresponding unphosphorylated peptide if no second unphosphorylated peptide has the same mass. Some phosphorylated peptides underwent

Reproduced with permission of the copyright owner. Further reproduction prohibited without permission.

β – eliminate reaction. A neutral loss H_3PO_4 (98 Da) from phosphorylated serine or threonine forms a α, β unsaturated bond and yields a residue of dehydroalanine (69 Da), or a residue of dehydroaminobutyric acid (83 Da). Thus, this 98 Da loss (or a multiple of 98 Da) also provided unequivocal identification of phosphorylated peptides containing serines and/or threonines. So far, twenty-one phosphorylation sites have been observed from a total of 74 serine and threonine residues of eIF4B protein. The phosphorylated sites can be assigned if all the serine and / or threonine residues are phosphorylated in each peptide. Ten phosphorylated sites were confirmed in deconvolution mass spectra, and seven phosphorylated sites could be possibly determined only in ion mass spectra due to their peptide ions were not transferred into deconlovolution mass spectra. Further confirmation needs to be done by tandem mass spectrometry. The other four phosphorylated sites in three peptides could not be assigned to exact positions, because each peptide contains more potential phosphorylation sites than observed phosphorylated site(s). Two dominant CKII phosphorylated regions were observed, which corresponded to NH_2-terminal residues 136-204 and COOH-terminal residues 395-444.

Reproduced with permission of the copyright owner. Further reproduction prohibited without permission.

ACKNOWLEGEMENTS

First, I greatly appreciate my mentor, Prof. Dixie J. Goss. She gave me an interesting project and excellent training in biochemistry and chemistry; she gave me good suggestions to solve problem and helpful discussion, guided me to finish this project and correct this dissertation.

I really appreciate Prof. Peter N. Lipke for suggestions about immunoblot, denature and second digestion of protein. I am grateful to Prof. Peter N. Lipke and Prof. Gary J. Quigley for reading of this manuscript and helpful discussion and correct this dissertation.

Finally, I really thank Prof. Karen S. Browning to provide wheat eIF4B plasmid DNA and anti-recombinant 4B antisera and Dr. Clifford E. Soll for mass spectra.

Reproduced with permission of the copyright owner. Further reproduction prohibited without permission.

TABLE OF CONTENTS

Reproduced with permission of the copyright owner. Further reproduction prohibited without permission.

Reproduced with permission of the copyright owner. Further reproduction prohibited without permission.

Reproduced with permission of the copyright owner. Further reproduction prohibited without permission.

LIST OF TABLES

LIST OF FIGURES

Reproduced with permission of the copyright owner. Further reproduction prohibited without permission.

Reproduced with permission of the copyright owner. Further reproduction prohibited without permission.

CHAPTER 1

The Translation Initiation Factor eIF4B Protein

1. Introduction of eIF4B protein

In wheat the process of mRNA binding to 40S ribosome is complex. Previous studies (1, 2, 3) have shown that eukaryotic initiation factor eIF4B could help eIF4F bind to the cap structure m^7GpppN at the 5' end of nuclear transcribed mRNAs. Subsequently eIF4A and eIF4B bind to the 5'-untranslated region. The eIF4B cooperates with eIF4F and eIF4A to unwind proximal secondary structures depending on the energy from ATP hydrolysis and create a single stranded mRNA region for 40S ribosomal binding.

Wheat eIF4B is a phosphoprotein that is composed of several isoelectric isoforms, similar to eIF4B from mammalian cells. The phosphorylation state undergoes dramatic changes during plant growth and development. The changes have been detected during different developmental stages, which correspond to different activities of protein synthesis, suggesting it is developmentally regulated. During the early development of seed, acidic isoforms of eIF4B change from degradation of isoforms are followed by the appearance of highly phosphorylated forms. The bulk of protein synthesis occurs. eIF4B undergoes gradual dephosphorylation during the late seed development, which correlates with the decline in protein synthesis. eIF4B phosphorylation increases during wheat germination. The more highly phosphorylated state is observed in the shoot, and largely predominates in both roots and leaves. The level of phosphorylated protein correlates with level of protein synthesis in wheat (4). eIF4B undergoes rapid dephosphorylation in leaves following a heat shock, and its loss correlates with the repression of translation (5).

Reproduced with permission of the copyright owner. Further reproduction prohibited without permission.

Wheat eIF4B is functionally similar to the 80-Kda initiation factor 4B from mammalian cells. Studies of mammalian eIF4B give further evidence of a relationship between the phosphorylation state and translational activity. The dephosphorylation of mammalian eIF4B occurred in the following: heat shock (6), serum depletion (7), or mitosis (8), which cause a reduction in translation, whereas an increase in phosphorylation of eIF4B by insulin stimulation correlates with an increase in translation (9).

To understand more fully key roles of phosphorylation of eIF4B in regulation of protein synthesis during developmental states and in response to various stimuli and signal transduction, it is necessary to determinate the phosphorylated sites. Radioactive phosphorus is only very poorly taken up by germinating seeds or growing plants. It is very difficult to obtain detectable amounts of labeled peptides using [^{32}P]-γ-ATP and separate the peptide mixture by excision of two dimension spots or HPLC column for Edman sequencing. The number of phosphorylation sites and the exact location of these sites in *vivo* and *vitro* were not reported. Mass spectrometry is an extremely useful method for determination of phosphorylated peptides and sites. It has several advantages over other techniques. It is very accurate, eliminates ambiguity by defining the site of phosphorylation. No radioactivity is required for this detection. It is very fast. In this project we did an approach to phosphorylated peptide and site analysis of wheat eIF4B. It consists of three steps: (1) A recombinant eIF4B protein was expressed in *E. coli*, and purified to obtain unambiguous one band of eIF4B. (2) Isolate phosphopeptides from a peptide mixture digest by immobilized metal affinity column (Fe(III)-IMAC). (3) Determine the phosphorylated peptides and sites by HPLC and on-line electrospray

Reproduced with permission of the copyright owner. Further reproduction prohibited without permission.

ionization mass spectrometry (ESI-MS) in combination with the known sequence of eIF4B peptides.

2. Materials and Methods

1.) Construction of a wheat eIF4B expression plasmid

The eIF4B plasmid used in these studies was provided by Dr.Karen Browning. An 849 bp BamHI / PvuII restriction fragment from the genomic clone encompassing the 5' half of the eIF 4B coding region and an 830 bp PvuII / NcoI restriction fragment from the cDNA encompassing the 3' half of the eIF4B coding region were ligated and inserted into restriction enzyme sites BamHI and NcoI of the pET-3d expression vector (10)

2.) Extraction of eIF4B Plasmid DNA

pET System is very good for the cloning and expression of recombinant protein in *E. coli.* The target genes are cloned under the control of the T7 promoter, which is not recognized by *E.coli* RNA polymerase and is specific to only T7 RNA polymerase. The eIF4B/pET3d plasmids were transferred into a expression host, BL21(DE3)pLysS (Novagen), which bears the T7 RNA polymerase gene in DE3 lysogen for expression of eIF4B protein. The T7 RNA polymerase is activated by addition of IPTG. In the host pLysS plasmids encode T7 lysozyme, a natural inhibitor of T7 RNA polymerase, which decreases transcription of genes in uninduced cells but does not interfere with induction by IPTG, so lowers the background expression level of the eIF4B gene.

The eIF4B/pET3d plasmid was transformed to *E. coli* BL21(DE3)pLysS competent cells.

Transformation Protocol:

(1.) Put sterile polypropylene culture tubes (Falcon 2059) on ice. This kind of tube results in efficient heat-shock treatment of the cells.

Reproduced with permission of the copyright owner. Further reproduction prohibited without permission.

(2.) Removed Competent Cells from –70 ^{0}C and placed on ice. Once the Competent Cells thawed, immediately gently flicked the tube, and quickly transferred 100 ul to each of the cold culture tubes kept on the ice.

(3.) Added 1 ul of eIF-4B DNA and 1 ul of control DNA respectively to per 100 ul of Competent Cells, and quickly gently mixed the tubes

(4.) Immediately put back the tubes into ice for 10mins.

(5.) Placed the tubes in water bath at exactly 42 ^{0}C without shaking for 45-50 seconds.

(6.) Put back the tubes into ice at once for 2 mins

(7.) Added 900 ul of SOC medium (4 ^{0}C) to each tube above, and incubated at 37 ^{0}C for 60 mins with shaking (approximately 225 rpm).

(8.) Diluted the cells 1:2 and plated 200 ul and 20 ul respectively on Amp plates, incubated the plates at 37 ^{0}C for 14 hours.

Many single colonies were shown on the plates.

3.) Purification of eIF4B Plasmid DNA

The buffer for Purification of eIF4B Plasmid DNA came from QIAprep Plasmid Kits.

Buffer P1: 50 mM Tris.Cl, pH 8.0, 10 mM EDTA, 100 ug/ml RNase A

Buffer P2: 200 mM NaOH, 1% SDS (w/v)

Buffer N3, PB and PE are proprietary formulations of QIAGEN and therefore the composition is unavailable, but indicted that N3 contains guanidine hydrochloride, acetic acid, and PB contains guanidine hydrochloride, isopropanol.

The method to purify plasmid DNA from bacteria was provided by the QIAprep Miniprep Hand-book. In this method, six independently transformed bacterial colonies

Reproduced with permission of the copyright owner. Further reproduction prohibited without permission.

were picked. These colonies were grown separately in 5 ml cultures. Plasmid DNAs were isolated from each culture. This methods involves the following steps:

Procedure:

(1.) Picked single colony, grow in 5 ml of culture media for 16 hours

(2.) Harvest and lyse the bacteria

a. Cells were harvest at speed (13000 rpm) in a conventional, table-top microcentrifuge, and pelleted bacterial cells were resuspended in 250 ul of Buffer P1 in which RNase A has been added, and transferred to a microfuge tube. No cell clumps should be visible.

b. 250 ul of Buffer P2 were added and gently inverted the tube 4-5 times to mix for 4 mins. The solution became viscous and slightly clear. The bacterial cells were lysed in Buffer P2, releasing the 4B plasmid DNAs. The optimized lysis time allows maximum release of plasmid DNAs without release of chromosomal DNA, while minimizing the exposure of the plasmid to denaturing conditions.

(3.) Purification of plasmid DNA

a. 350 ul of Buffer N3 were added and the tube inverted immediately, but gently, 4-6 times. The solution became cloudy and very viscous. The Buffer N3 neutralizes and adjusts lysate to high salt conditions. The high salt concentration causes denatured proteins, chromosomal DNA, cellular debris, and SDS to precipitate, while the shorter plasmid DNA renatures correctly and stays in solution.

b. The solution was centrifuged for 10 mins at speed (13000 rpm). The eIF-4B plasmid DNAs remained in the clear supernatant, and the supernatants was applied

Reproduced with permission of the copyright owner. Further reproduction prohibited without permission.

to the QIAprep column, centrifuged for 50 seconds. The flow- through was discarded.

c. The QIAprep spin column was washed with 0.5 ml Buffer PB and centrifuged for 50 seconds. Only DNA was adsorbed, while RNA, cellular proteins, and metabolites were not retained on the membrane of the column and were found in the flow- through, which was discarded..

(4.) The QIAprep spin column was washed with 0.75 ml Buffer PE which efficiently washed salts away from the QIAprep spin column and the column was centrifuged for 50 seconds. The flow- through was discarded.

(5.) The column was centrifuged again for 1 min to remove residual wash buffer. Residual ethanol from Buffer PE may inhibit subsequent enzymatic reactions.

(6.) Pure 4B plasmid DNA was eluted from the QIAprep column with 50 ul of 10 mM Tris-HCl, pH 8.5 by centrifuging for 1min.

4.) Identification of Bacterial Colonies that contain eIF-4B Recombinant Plasmids

There is a method that is commonly used to identify bacterial colonies that contain recombinant plasmids: **Restriction analysis of small-scale preparations of plasmid DNA**

In this method, plasmid DNAs isolated from each culture by the method previously described in this chapter were analyzed by double digestion with restriction enzymes Hind III (Promega) and Xbal (BioLabs) or BamH I (BioLabs) and Xbal, and eletrophoresis on 0.8 % agarose gel.

Prepare the control reaction as indication below:

2 ul of eIF4B plasmid DNA from Karen S. Browning's Lab

Reproduced with permission of the copyright owner. Further reproduction prohibited without permission.

1 ul of 10x NE Buffer 2 (50 mM NaCl, 10 mM Tris-HCl, 10 mM $MgCl_2$, 1 mM dithiothreitol)(BioLabs)

1 ul of BamH I (20 u/ml)

1 ul of Xbal (20 u/ml)

Then added dH_2O to a final volume of 10 ul

Prepare two sample reactions as indication below:

2 ul of isolated plasmid DNA

1 ul of 10x NE Buffer 2

1 ul of Hind III (20.00 u/ml)

1 ul of Xbal (20.00 u/ml)

The second reaction contained the same except BamH I (20.00 u/ml) instead of Hind III. Both control and sample reactions were incubated at 37 ^{0}C for 1 hr, then run 0.8% agarose gel.

5.) Purification of eIF4B protein

eIF4B protein was purified by 5 ml HiTrap SP column (Amersham Pharmacia Biotech) and Bio-Gel-P- 60 size exclusion column (BIORAD).

One liter of (LB) culture medium innoculated with eIF4B cells was grown at 37^0 C to an A_{600} of 0.3. Isopropyl-β-D- thiogalatopyranoside (IPTG) was added to a final concentration of 1 mM and the culture incubated with shaking for 4 hr at 37 ^{0}C. Harvested cells were sonicated in 6 ml buffer B-600 (20 mM HEPES/KOH, pH 7.6, 0.1 mM EDTA, 1.0 mM DTT, 10% glycerol and 600 mM KCl) containing 100 μg/ml soybean trypsin inhibitor, 2.0 μg/ml aprotinin and 1.0 mM phenylmethylsufony fluoride (PMSF). The cell lysate was centrifuged at 1500 rpm for 10 min at 4 ^{0}C. The supernatant

Reproduced with permission of the copyright owner. Further reproduction prohibited without permission.

was removed from the ribosomes by ultra-centrifugation at 4200 rpm for 2 hr. The supernatant was diluted to 60 ml and loaded onto a 5 ml HiTrap SP column (Amersham Pharmacia Biotech) equilibrated in buffer B-60, washed with buffer B-60 until the A_{280} reached baseline, and eluted with a 30 ml linear gradient from 60 to 600 mM KCl in buffer B in a cold box. The fractions contained partial purified eIF4B protein, and were pooled and run on a HiTrap SP column one more time.

The fractions containing purified 4B protein were pooled and concentrated by the Centriplus YM-30 Centrifugal Filter Device at 4000 rpm for 1-2 hr at 4 ^{0}C, and run on a Bio-Gel-P-60 size exclusion column (50-ml bed volume) (BIORAD) equilibrated with buffer (10 mM Tris.Hcl, 10 mM KCl, pH 7.25). Approximately 1.0 mg recombinant eIF4B protein was purified from a 2 L *E.coli* culture. The sample fractions were electrophoresed on a 10% SDS-PAGE gel and visualized by staining with Coomassie Blue.

6.) Immunoblot of eIF4B protein

For immunoblots, briefly, the proteins were transferred overnight to nitrocellulose membranes from SDS gels. The membranes were blocked with 3% gelatin in buffer (140 mM NaCl, 10 mM tris. pH 7.4) and incubated in the same buffer with 1% gelatin and a 1: 500 dilution of the recombinant eIF4B antibody provided by Karen S. Browning's Lab (10), followed by a 1:1000 dilution of anti-rabbit lgG HRP (Promega). Color was developed with 15 ml of 4-chloro-1-naphthol (SIGMA) with 60 ul of 3% H_2O_2 (SIGMA).

3. RESULTS AND DISCUSSION

Identification of eIF-4B Recombinant Plasmid DNA

Reproduced with permission of the copyright owner. Further reproduction prohibited without permission.

The bands shown on agarose DNA gel correspond to molecular weights of fragments of eIF-4B Recombinant Plasmids (Table 1-1 and Figure 1- 1). In figure 1-1, Lane 1, the DNA ladder; Lane 2, the sample was doubly digested with Hind III and Xba I but was not completely digested because the top band didn't completely disappear, which corresponded to the molecular weight of intact eIF-4B Plasmid (6317) consistent with highest band of control eIF-4B Plasmid. The other two bands correspond to molecular weights of fragment of eIF-4B Plasmid (2238, 4079). Lane 3, sample was almost completely digested by BamH I and Xba I, and two bands correspond to molecular weights of fragments of eIF-4B Plasmid (4560, 1759). Lane 4, Karen Browning's sample as a control was almost completely digested by BamH I and Xba I, and the molecular weights of two fragments were consistent with sample 3; therefore bacterial colonies contained eIF-4B recombinant plasmid DNA.

Purification and Identification of recombinant wheat eIf-4B Protein

The purified recombinant eIF4B protein is shown in Figure 1-2. To determine that the purified recombinant polypeptide was in fact eIF4B, immunoblots were performed. The rabbit anti-recombinant 4B antisera were not affinity purified, and there are cross-reacting *E. coli* antibodies. The unpurified antiserum was directly used as antibody in control of sample [1] and [2]. The samples were as the follows: [1] putative purified protein, [2] cellular extracts from nonexpressing cells and [3] extract from eIF-4B expressing cells. The eIF4B should be in the purified material [1] and in the extract from expressing cell [3], but not in the extract from non-expressing cells [2] (Figure 1-3).

Reproduced with permission of the copyright owner. Further reproduction prohibited without permission.

CHAPTER 2

The eIF4B Protein Phosphorylation

1. Introduction of Protein Phosphorylation

Phosphorylation of serine, threonine and tyrosine residues is one of the most important modifications of proteins. During protein phosphorylation, phosphates from the chemical energy-carrying adenosine triphosphate (ATP) molecules are transferred to the hydroxyl group of the respective serine, threonine or tyrosine residues by protein kinases. Protein phosphatases make this process reversible, in which phosphates are removed, hydrolysis occurs and protein switch back to its original conformation as shown in Figure 2-1. If a protein is controlled by its phosphorylation state, the kinases and phosphatases could directly affect activity of this protein. For their discovery of reversible protein phosphorylation as a biological regulatory mechanism, in 1992 Edmond H. Fischer and Edwin G. Krebs were awarded the Nobel Prize for Physiology and Medicine.

Reversible phosphorylation has been known to control a wide range of biological functions and activities (11-14). Previous studies have established that the changes of eIF4B phosphorlation state corresponded to different activity of protein synthesis and various stimuli (4,5,6,7,8,9) To understand phosphorylation function we have to know phosphorylation sites of proteins. The particular residues phosphorylated on a protein can provide information how the protein activity is regulated and which enzymes are responsible for the regulation and the mechanism of phosphorylation in response to various stimuli in signaling pathway.

2. Significance

Reproduced with permission of the copyright owner. Further reproduction prohibited without permission.

Wheat eIF4B is multiple phosphorylated *in vivo.* Its phosphorylation state depends on the development stage, and correlates with changes in protein synthesis (4, 5). eIF4B is normally phosphorylated in developing seeds and actively growing leaves that have high levels of protein synthesis, but undergoes dephosphorylation during late seed development when protein synthesis is repressed (4). eIF4B became dephosphorylated in response to heat-shocked (5). The hypophosphorylated eIF4B can be phosphorylated by a high level of CKII (4, 5). Native (phosphorylated) eIF4B is greater than 14-fold more effective in its functional interaction with phosphorylated poly (A)- binding protein (PABP) than recombinant (nonphosphorylated) eIF4B. Native eIF4B enhanced greatly the RNA-binding activity of phosphorylated PABP whereas it had less effect on the poly (A)- binding activity of hypophosphorylated PABP. Recombinant eIF4B was more effective in stimulating the poly (A)-binding activity of hypophosphorylated PABP but less effect on phosphorylated PABP to poly (A) RNA. Phosphorylated eIF4B preferentially associates with polysomes relative to recombinant eIF4B (15). These data implicated the eIF4B phosphorylation plays a possible important role in plant growth processes.

Phosphorylation sites of proteins have been an essential step in the analysis of control of many biological systems. The phosphorylated sites could be mutated, in which target serine or threonine residues are substituted with either alanine or glutamate. The functional significance of phosphorylation sites could be investigated in interactions between eIF4B and other initiation factors, mRNA, PABP, PABP-poly (A) and DNA, respectively and determine which of phosphorylation sites are functionally important.

Reproduced with permission of the copyright owner. Further reproduction prohibited without permission.

3. Materials and Methods

1.) Phosphorylation and Digestion of wheat eIF4B Protein

eIF4B protein was phosphorylated in vitro by Casein Kinase II (New England BioLabs). Casein Kinase II can phosphorylate serine and threonine residues.

500 µl of purified eIF4B at concentration of 0.40 mg/ml were incubated in CKII buffer containing 20 mM Tris.HCl, 50 mM KCl, and 10 mM $MgCl_2$, pH 7.5 in a final volume 0.55 ml at 31 ^{0}C for 3 hr in the presence of 4 mM ATP and 3000 µ of CKII. The phosphorylated and unphosphorylated eIF4B were electrophoresed on a 10% SDS-PAGE gel for 3 hr and visualized by staining with Coomassie Blue.

50 mM EDTA, 2 M urea was added to the phosphorylated eIF4B for 30 min, then dialyzed in 0.05 M NH_4HCO_3, 2 mM $(NH_4)_2HPO_4$, 2 M urea, pH 8.0 for 6 hr, and digested with enzyme trypsin (SIGMA) at a ratio of 20:1 (W:W, protein:enzyme) at 37 ^{0}C for 7 hours.

2.) Enrichment of Phosphopeptides from wheat eIF4B

1 ml of Sepharose Fast Flow column (Amersham Pharmacia Biotech) was used to enrich phosphopeptides. The column was washed with 6 ml of distilled water, followed by 15 ml of loading buffer consisting 0.1 M acetic acid (pH 3.3). The column was activated with Fe (III) ions by introducing 4 ml of 30 mM $FeCl_3$ in the loading buffer at 400 µl /min through the column. The excess Fe^{3+} ions were washed away by passing 30 ml of loading buffer, followed by 8 ml of 0.1 % NH_4Ac, pH 8.0, then re-equilibrate the column with 10 ml of loading buffer before sample was loaded.

The peptide sample (200 µg, 0.54 ml) was acidified with 1 M acetic acid, and an aliquot was loaded onto the Fe (III)-IMAC column. The column was washed with 5 ml of

Reproduced with permission of the copyright owner. Further reproduction prohibited without permission.

loading buffer. The peptides were eluted with 20 ml of 0.1% NH_4Ac, 2 mM $(NH_4)H_2PO_4$ pH 8.0. Both loading and eluting buffer were introduced into the affinity column at a flow rate of 0.2 ml/min. The progress of this separation was monitored at 280 nm. A second digestion was performed to avoid incompletely digested peptides. The eluate was lyophilized, digested again with trypsin at a ratio of 30:1 (W:W, protein:enzyme) for 4 hour at 37 ^{0}C, and was directly analyzed by HPLC-ESI/MS.

4. Results and discussion

Phosphorylation of wheat eIF4B Protein

Wheat eIF4B has been previously shown (4,5) to be a phosphoprotein *in vivo*. The protein was treated *in vitro* by CKII in buffer (20 mM Tris.HCl, 50 mM KCl, and 10 mM $MgCl_2$, pH 7.5) with and without ATP at 31 ^{0}C for 3 hr. The phosphorylated and unphosphorylated eIF4B were electrophoresed on a 10% SDS-PAGE gel for 3 hr and visualized by staining with Coomassie Blue as shown in Figure 2-2 which provided an identification of modifying the eIF4B by high level of protein kinases CKII. The phosphorylated band of eIF4B is a little higher than the corresponding unphosphorylated band on a 10% SDS-PAGE gel.

Enrichment of Phosphopeptides from wheat eIF4B

Many phosphoproteins are present in the cell at relative low concentrations. Individual phosphorylation sites exist in very low abundance. The phosphorylated protein may have different forms (increase of 80 Da or loss of 98 Da) (16, 17). This causes detection to be more difficult. In the mass spectrometric analysis of phosphopetides, an inherent difficulty is that a large number of nonphosphorylated peptides in complex peptide

Reproduced with permission of the copyright owner. Further reproduction prohibited without permission.

mixtures often suppress ionization of phosphopeptides and lead to poor ionization efficiency (18). Ionization of the phosphopeptide itself was also suppressed by itself due to the phosphate group with two negative charges. If the phosphorylation degree is low, it is extremely difficult to detect the phosphorylated peptide ion signals from a large number of unphosphorylated peptides. In such case, phosphopeptides need to be enriched prior to HPLC/ESI-MS analysis. An effective method is the removal of interfering components by immobilized metal ion affinity chromatography (IMAC). This method exploits the relatively high affinity of phosphate for Fe (III) (19, 20, 21, 22 and 23). The metal cation in an IMAC column acts as an electron acceptor. Negatively charged phosphate groups bind the chelated metal Fe ion and are retained on the column, but the peptides containing a high content of acidic residues also can nonspecifically bind Fe ions. Therefore, peptides isolated in this manner can not be expected to represent only phosphopeptides, However, this approach can simplify the analysis of mass spectra by excluding many non-phosphopeptides and reducing possible ion suppression effects. The Fe affinity chromatography separation yielded two peaks. The first one was due to the components that did not interact with the column and the second was due to those components retained in the column. The column was eluted with 2 ml of eluting buffer as shown in Figure 2-3.

Reproduced with permission of the copyright owner. Further reproduction prohibited without permission.

Chapter 3

Electrospray Ionization Mass Spectrometry (ESI/MS)

1. Introduction of ESI/MS

Mass Spectrometry is a rapid, very sensitive and effective technique for analyzing microgram quantities of sample. It has been widely used to identify unknown organic compounds, biopolymers, peptides and proteins. It is also used to measure the quantity of known compounds. A mass spectrometer is an instrument that can separate charged molecules according to their mass to charge ratio and exhibits multiply charged state of ions of the same molecule and location of the multiply charged state in mass spectrum, and obtains high accrual molecular weight. It becomes a useful tool in biochemical analysis. It is used to identify post-transtionally modified proteins, such as phosphorylation, glycosylation and sulfation. It is also applied in studying protein conformation, stability of proteins and molecular interactions.

To perform direct MS measurements on proteins and peptides successfully, the MS ionization technique must satisfy the following criteria: (a) the electrospray ionization method must generate intact multiply charged gas-phase protein or peptide ions directly from solution; (b) the energy which the molecules of proteins or peptides obtain during the ionization process must be low enough to prevent dissociation of the complex and let the weakly bound complexes be detected; and (c) the MS instrumentation must have a sufficient range of mass-to-charge (m/z) to observe the ionized complex. Electrospray ionization (ESI) is much better than other soft ionization methods for small amounts of nonvolatile peptides, protein, and polymers. The technique is carried out at atmospheric

Reproduced with permission of the copyright owner. Further reproduction prohibited without permission.

pressure. Figure (3-1) shows a schematic diagram of a mass spectrometry.

The liquid sample comes from a liquid chromatography systems such as HPLC, passes through a small stainless metal needle. Values of applied voltage at the needle are several kilovolts (e.g. 4500). A high electric field at the needle tip charges the surface of the emerging liquid, the liquid pushes out of the needle tip and forms many finely charged droplets, this technique is known as electrospray. This method for droplet generation has been used in various applications since the early part of the 1900s. Driven by the electric field the droplets move towards the inlet of the glass capillary through warm nitrogen gas flow, which helps solvent and other uncharged molecules rapidly evaporate. The charged droplets get smaller, the charge density increases, and the increasing coulombic repulsion within the droplets come to exceed the surface tension so that droplets disintegrate and release droplets containing desolvated ions in the gas phase. The capillary, skimmer in the first vacuum chamber, as efficiently as possible, emerge only one solute molecule ions into a second vacuum chamber containing a quadrupole mass analyzer (24, 25 and 26). The mass analyzer is most widely used for LC-MS instrumentation to separate ions within a selected range of m/z ratios. The analyzer is an important part of the instrument because of the role it plays in the instrument's accuracy and mass range. A detector measures ion abundance. The result of ionization, ion separation, and detection is a mass spectrum that can determine the molecular weight. Mass measurement accuracy as high as 0.01% is possible with this technique. The essential features of ESI Mass Spectrometer include the five same basic parts as any mass spectrometer: a sample introduction device, an ionization source, a vacuum system, a mass analyzer and an ion detector.

2. Features of Electrospray Ionization Mass Spectrum

Reproduced with permission of the copyright owner. Further reproduction prohibited without permission.

An ESI- mass spectrum generally consists of a distribution of multiply charge molecular states and a single maximum charge state for protein. The ions carrying multiple charges are the most obvious feature of an ESI- mass spectrum. This reduces their mass to charge ratio compared to singly charged species and thus multiplies the effective mass range of any analyzer by the number of charges per ion. This allows mass spectra of large molecules to be obtained. These ions are easily detected due to multiple charges. ESI is a gentle ionization method. No peptide bonds dissociate for protein (27, 28). The charge states for protein are generally from proton noncovalent attachment, and adjacent peak always appear to vary by addition (in positive mode) or subtraction (in negative mode) of one charge. A feature of ESI mass spectra for most proteins is that the average charge state increases in an approximately linear fashion with molecular weight (29, 30, 31) It has been suggested that the number of positive charges is generally related to the number of basic residues (Arg, Lys, His, NH_2-terminus) on the molecule in positive ion mode (32, 33). The highest charge states observed for small proteins and peptides are consistent with this explanation (29, 30, 31) but a few exceptions exist. Deprotonation occurs at acidic residues (Asp, Glu, Tyr, COOH-terminus) in negative ion mode.

3. Molecular Weight Determination

1). Averaging algorithm

Shown below a typical positive ion ESI mass spectrum of a peptide (residues 23-47) of eIF4B.

Reproduced with permission of the copyright owner. Further reproduction prohibited without permission.

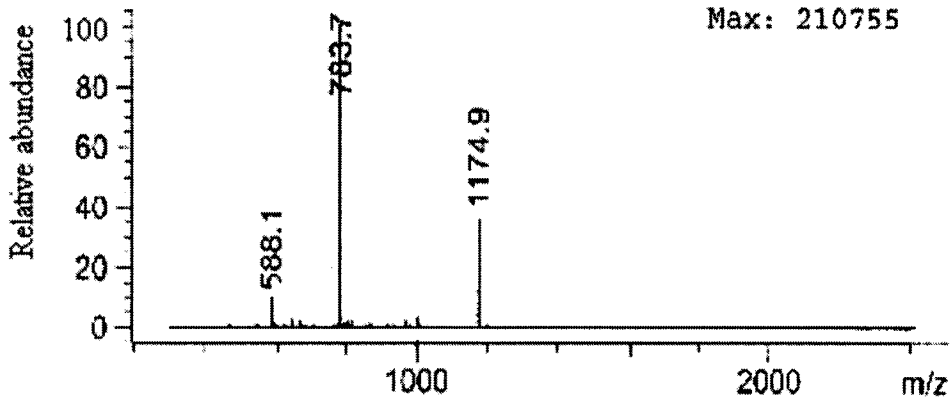

The spectrum contains a set of peptide ions at a range of charge and each is assigned to the same molecule. The most abundant ion is taken as 100% (base peak). The other ion abundances are expressed as a percentage of the largest signal ion. The total number of ion counts detected for the highest peak is given in the top right hand corner (34).

The change number of the peptide ions may be immediately determined from the spectrum above (35, 36) given several assumptions.

One may assume the three peaks shown in the above mass spectrum are related (charged variants of the same molecule), and assume that they differ by a single charge. For protein molecules the charging is often due to proton attachment to them. The equation (1) and (2) describes the relationship between charge (z) and molecular mass (m) of a multiply charged ion at m/z

$$m = 1174.9z \quad (1)$$

$$m + 1 = 783.7(z+1) \quad (2)$$

Since m is assumed to be the same for both peaks, we can set these two equations equal to each other and solve for the charge state of the peaks.

$$1174.9z = 783.7(z+1) - 1$$

Reproduced with permission of the copyright owner. Further reproduction prohibited without permission.

$$z = 2$$

This tells us that the two peaks in the spectrum are mathematically related. The charge number of the peak at m/z 1174.9 is +2. The charge number is therefore +3 for the peak at m/z 783.7 and +4 for the peak at m/z 588.1.

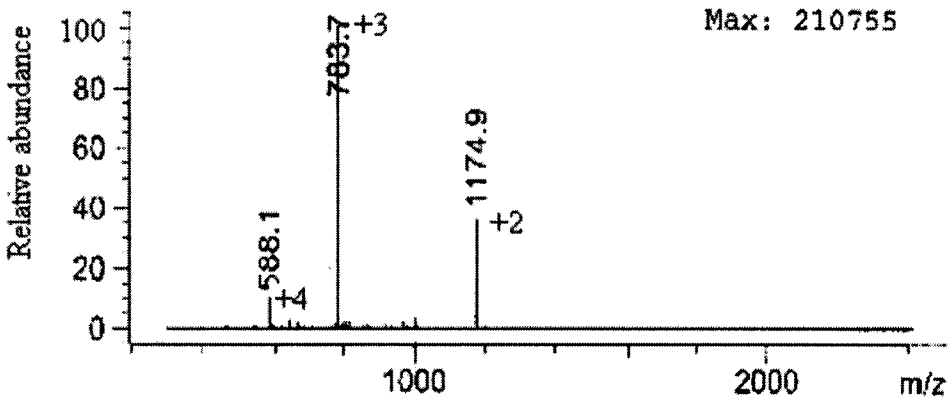

b. Determining the average mass of a peptide

Once the charge states of peaks are determined a mass can be calculated by hand. You can think of the three peaks in the spectrum as separate mass measurements of the same molecule, and average the three resulting values to get an accurate assessment of the mass.

Charge State	Calculation	Unprotonated Mass (M)
+2	m/z = 1174.9 = (M+2H)/2	2347.8
+3	m/z = 783.7 = (M+3H)/3	2348.1
+4	m/z = 588.1 = (M+4H)/4	2348.4
		average: 2348.1
		theoretical: 2348.17

Reproduced with permission of the copyright owner. Further reproduction prohibited without permission.

2). Deconvolution algorithm

The "deconvolution algorithm" mathematically transforms each set of multiply charged ions with relative abundance versus mass to charge ratio in ion mass spectrum into a single peak corresponding to a molecular mass of the component with relative (or absolute) abundance versus mass in the deconvolution mass spectrum. This "Deconvolution algorithm" has been programmed. The process is as follows:

a. Determine the exact site of each ion in the spectrum.
b. Determine which ions correspond to the same component. A series of consecutive charge numbers corresponding to a set of ions is applied to determine whether they give the same molecular weight. The ions with the same molecular weight are presumed to be from the same component.
c. Transform m/z values of each ion of a set for each component to the corresponding mass values, resulting in one peak per component with mass vs. abundance.
d. Apply a curve-fitting algorithm to this peak for the actual molecular weight assigned to the component.

The software can determine the average molecular weight of each component in the sample. It can also find the charge state of each peak in the charge- state envelope of a given compound. Deconvolution algorithm has been well developed to resolve multiple compounds in the complex mixtures.

4. High Performance Liquid Chromatography/Mass Spectrometry

Sample separation and all mass spectra were accomplished using an Agilent 1100 LC/MSD system. The partial purified phosphopeptides were separated by reversed-phase

Reproduced with permission of the copyright owner. Further reproduction prohibited without permission.

HPLC on a C_8 column (2.1x150 mM) with an acetonitrile gradient in 0.5% (V/V) acetic acid (solvent A). Elution was performed with the following gradient: 0 -100 % solvent B (95% acetonitrile (V/V) in 0.5% (V/V) acetic acid) over 40 min at a flow rate of 400 µl/min. The electrospray was carried out using the capillary held at 4500 volts (positive) with pneumatic assistance of nitrogen gas. ESI/MS analysis was performed using a single quadrupole electrospray ionization mass analyzer with full scan between m/z 400 and 2400. The raw data was analyzed on the deconvolution module of the HP Chemstation software for unambiguous assignment of molecular weights.

In the negative-ion ESI/MS analysis, elution was performed with the following gradient: 0-100% solvent B [60% acetonitrile (V/V) in 40% solvent A (5 mM NH_4Ac pH 6.5)] over 40 min at a flow rate of 400 µl/min. The needle tip was held run at voltage of 4000 volts (negative). Mass spectrum analysis was performed using a single quadrupole electrospray ionization mass analyzer with full scan at m/z 300 to 2400.

5. RESULTS AND DISCUSSION

1.) Identification of phosphorylated peptide

Phosphorylated peptides were identified by analysis of a trypsin digest from total mixture of IMAC retained peptides or from fractions of IMAC run on reverse-phase HPLC coupled on line ESI/MS. The HPLC allowed removal of some of the background signal resulting from the Fe- IMAC elution conditions and the sample was further separated by HPLC prior to ESI-MS. Utilizing IMAC and HPLC columns avoided ion suppression effects and resulted in significant improvements in detection sensitivity

Reproduced with permission of the copyright owner. Further reproduction prohibited without permission.

compared to a single column, thus simplifying interpretation. The on-line data provided mass ion spectra and deconvolution mass spectra at different HPLC elution times. HPLC/ESI-MS peptide mapping can be used to determine phosphorylation peptides in cases where each peptide sequence is known in a database (Agilent Technologies Peptide Tools). For purified protein digests, the phosphorylated peptide is confirmed by detection of the 80 Da (HPO_3) or a multiple of 80 Da difference between the observed mass of peptide and the calculated one on the basis of sequence if no second unphosphorylated peptide has the same mass (37, 38, 39 and 40). It should be noted that phosphoserine and phosphothreonine residues of phosphopeptides have a tendency to undergo a β-elimination reaction under basic conditions or collision in the gas phase in mass spectrometry, and generate a dehydroalanine (69 Da) and dehydroaminobutyric acid, (83 Da) respectively from a phosohorylated peptide that was 80 Da higher than the predicted mass.

The neutral loss of 98 Da has been shown to be very useful for the identification of the presence of phosphorylation of serine and / or threonine since H_3PO_4 loss is phosphopeptide-specific and often much more abundant than the other corresponding peptides (41, 42,43, 44 and 45). The mass values determined by 80 Da increase and loss of 98 Da is within a mass relative error $\leq$ 0.05% for determination of all of phosphorylated peptides of eIF4B protein.

Six peptides (Table 3-1) were confirmed as phosphorylated peptides in the deconvolution mass spectra. Two of them, residues 139-147 and 439-450 with another forms, appeared in only ion mass spectra (Table 3-2), and were not transferred to deconvolution mass spectra. Nine possible phosphorylated peptides (Table 3-2) with +1

Reproduced with permission of the copyright owner. Further reproduction prohibited without permission.

charge were observed in the ion mass spectra. All of the peptides with multiply charged ions or single charged ion in Figure 3-2A-22A, appeared in different time windows. The ion mass spectra in left panels were directly transferred to deconvolution mass spectra in right panels, such as in Figure 3-2B-7B, 9B, 12B, 16B, 18B and 22B, and were used to obtain the molecular weights of peptides, where the abundance of the peptides is taken to be the absolute abundance. The phosphorylated peptide is labeled (●) and the corresponding unphosphorylated peptide is labeled (■) at the top of each peak. Other mass peaks resulted from non-phosphopeptide of eIF-4B after IMAC column and from trypsin autolysis.

2.) Analysis of phosphorylated peptides

In the following section "P" designates phosphorylation of the following residue.

(1). Analysis of phosphorylated peptide IpSQMEK

The sample from total IMAC-retained peptides was analyzed by HPLC-ESI/MS. Multiply charged state of mass ion spectrum in Figure 3- 2A was transferred to the deconvolution mass spectrum shown in Figure 3-2B. The peak at 814.4 Da with relative abundance 15.56 of the largest signal peak is in excellent agreement with residues 433-436 (IpSQMEK) with one phosphorylated site at Ser^{434} (theoretical 734.4+80 = 814.4 Da) due to only one potential phosphorylation site in this peptide. The corresponding unphosphorylated peptide (theoretical 734.4) was not observed because only one glutamic acid residue. The peptide can not be retained on the IMAC column (19).

(2). Analysis of phosphorylated peptide: pSRPpSPFGAAKPR

The sample from total IMAC-retained peptides was analyzed by HPLC-ESI/MS. In Figure 3-3A, the peptide ions with single, double and triple charges ([MH^+ = 1332.7, [M

Reproduced with permission of the copyright owner. Further reproduction prohibited without permission.

$+ 2H]^{2+}$ = 666.9 and $[M + 3H]^{3+}$ = 445.0]) were detected and displayed the corresponding peak with mass of 1332.0 Da in deconvolution mass spectrum shown as Figure 3-3B. The mass represents a prominent loss of 98 Da from phosphorylated residues 284-295 pSRPpSPFGAAKPR (theoretical 1269.7 + 160 – 98 = 1331.7 Da), but we were unable to determine whether there was one specific site of a loss of 98 Da, corresponding to the dehydroalanine in this peptide or a mixed population of single dehydroalanine in the peptides, lose H_3PO_4 from different phosphorylated sites at Ser^{284} or Ser^{287}. This peptide was phosphorylated at Ser^{284} and Ser^{287} because there are only two serine residues in the peptide. It is possible that some of the peptides (theoretical 1269.7 Da) were not phosphorylated. Because the peptide contains no aspartate acid and glutamic acid residues, and has no affinity for the Fe (III)-IMAC their ions do not appear in the mass spectrum.

(3). Analysis of phosphorylated peptide: pSFpSPAPpTDpSGR

The sample from total IMAC-retained peptides was analyzed by HPLC-ESI/MS. The mass ion spectrum in Figure 3-4A yields six molecular masses in deconvolution mass spectrum shown in Figure 3-4B. The peak at 1279.8 Da with absolute abundance of 36385 was mass 160 Da higher than the calculated mass of residues 159-169 (SFSPAPTDSGR) (theoretical 1120.5 + 160 = 1280.5 Da), corresponding to addition of two phosphate groups. Three serine residues and one threonine residue are contained within the peptide, thus the two sites of phosphorylation cannot be assigned based on the molecular mass data. It was observed that this peptide was present in two forms, one with two phosphate groups and another one, eluted in a later HPLC fraction, shown in Figure

Reproduced with permission of the copyright owner. Further reproduction prohibited without permission.

3-5A and 5B. The peak at 1048.2 Da in Figure 3-5B was present with lower absolute abundance of 9444 corresponds to the predicted phosphorylated residues 159-169 with a loss of 4x98 Da (theoretical 1120.5+4x80-4x98 = 1048.5 Da). This may be explained as four phosphorylated sites of the peptides underwent a β-elimination reaction in the gas phase collision. This shows that three serines and one threonine at Ser^{159}, Ser^{161}, Thr^{165} and Ser^{167} can be phosphorylated. The peak at 1279.8 Da shows that most of the phosphorylated peptides contain only two phosphorylated sites. The corresponding unphosphorylated peptide (theoretical 1120.5 Da) was not shown in mass spectrum; with only single Asp residue, it should not be retained on the IMAC column (19).

(4). Analysis of phosphorylated peptide: LpSGPpSPLGR

The sample from total mixture peptides of IMAC run was analyzed by HPLC-ESI/MS. The peak at 1043.2 Da in Figure 3-5B corresponded to the predicted phosphorylated residues 173-181 (LpSGPpSPLGR) containing two phosphorylated sites at Ser^{174} and Ser^{177} (theoretical 883.5+160 = 1043.5 Da). The corresponding unphosphorylated peptide can not be retained on the IMAC column (19).

(5). Analysis of phosphorylated peptide: QLDLLpTVELDDK

The total mixture peptides of another IMAC run were analyzed by HPLC-ESI/MS. An unphosphorylated peptide with multiply charged states and mass of 1401.1 Da appeared respectively in Figure 3-6A and 6B due to both three Asp recidues and one Glu residue have affinity for the Fe (III)-IMAC (19). This mass corresponded to predicted residues 439-450 (QLDLLTVELDDK) (theoretical 1400.7 Da). In next HPLC fraction mass spectrum, the multiply charged state of mass ion spectrum shown in Figure 3-7A was transferred to deconvolution mass spectrum shown in Figure 3-7B and appeared a

Reproduced with permission of the copyright owner. Further reproduction prohibited without permission.

peak at 1383.6 Da corresponds to a prominent neutral loss of 98 Da from the residues 439-450 (QLDLLpTVELDDK) phosphorylated at Thr^{444} (theoretical 1400.7+80-98=1382.7). The relative error is 0.065% > 0.05%. The observed mass is 0.9 Da higher than calculated value (1383.6-1382.7=0.9 Da). Our mass accuracy for most peptides is usually ± 0.1–0.3 Da. The difference mass of 1.0 Da may suggest that Gln^{349} of this peptide is converted to Glu most likely due to deamidation reaction and the terminal amide group change into a carboxylate [(Q→E) LDLLTVELDDK]. In the same experiment the previous phosphorylated peptide IpS[(Q→E) MEK also occurred deamidation. A peak at 815.4 Da (theoretical 814.4) in deconvolution mass spectrum was observed. Another possible form of this peptide QLDLLpTVELDDK was found in fraction 7^{th} tube of another IMAC run and was observed only in mass ion spectrum (Figure 3-8A) and not in deconvolution mass spectrum. It is possible due to only single charge state or lower amplitude was detected. The peak ion at m/z 1481.6 present at 20.80% of the most abundant peptide is in good agreement with the predicted phosphorylated peptide with charge + 1 at m/z 1481.7. The ion was not observed in multiply charged states of mass ion spectra of unphosphorylated protein digest. The observed mass of 1480.6 Da (MH^+-H^+=1481.4-1) matches with the predicted mass (1480.7 Da) corresponding to residues 439-450 (QLDLLpTVELDDK) with an additional 80 mass units at Thr^{444}, thus the peptides containing Thr^{444} were present in two forms, one with phosphate and anther with dehydroalanine.

(6). Analysis of phosphorylated peptide: DpSDLDMPpSR

The mass spectrum shown in Figure 3-9A, 9B results from analysis of peptides in the 8^{th} tube of IMAC run. The peak at 1016.5 Da in deconvolution mass spectrum (Figure3-

Reproduced with permission of the copyright owner. Further reproduction prohibited without permission.

9B) corresponds to a neutral loss of 98 Da from the residues 139-147 (DSDLDMPSR) with one phosphorylated site (theoretical 1034.4 + 80 – 98 = 1016.4 Da). This peptide was present in the other two forms, one with two phosphate groups did not exist in the 8th tube, and appeared in the 7th tube of IMAC fraction and shown in mass ion spectrum (Figure 3-10A). The peak at m/z 1195.7 with lower abundance could be assigned to the same residues 139-147 with two phosphorylated sites corresponding to predicted phosphorylated peptide ion (theoretical MH+ = 1035.4+2x80 = 1195.4). A peak at m/z 1098.0 corresponding to a prominent neutral loss of 98 Da from 1195.7 Da was observed in next eluting HPLC fraction shown in mass ion spectrum (Figure 3-11A). The corresponding unphosphorylated ions appeared at m/z 1035.5 shown in another time HPLC-ESI/MS analysis in Figure 3-12A and 12B, but the phosphorylated ions didn't appear in that experiment. The experimented data confirm that the peptide was phosphorylated with three possible forms: one with one dehydroalanine, one with two phosphate groups and one with both a phosphate and a dehydroalanine. Each of the two potential phosphorylation sites Ser^{140} and Ser^{146} has chance to obtain phosphate group.

(7) Analysis of phosphorylated peptide: GSFGGGGSSDR

The mass ion spectrum shown in Figure 3-13A resulted from fraction 7th tube of an IMAC run. The ion at m/z 1143.0 present at 51.0% of the most abundant peptide corresponds to the predicted residues 510-520 (GSFGGGGSSDR) with two phosphorylated sites with charge +1 at m/z 1143.4 (theoretical 983.4+160=1143.4). In another analysis of total peptide mixture after IMAC run, this peptide ion was present another form, with one phosphorylated site shown in Figure 3-14A. The peak ion at m/z 1062.9.0 present at 7.8% of the most abundant peptide and the peak ion at m/z 531.9

Reproduced with permission of the copyright owner. Further reproduction prohibited without permission.

(expanded Figure 3-14A) with 1.02% of the most abundant peptide correspond to the predicted phosphorylated peptide with charge +1 at m/z 1063.4 and with charge +2 at m/z 532.2, respectively. The observed average mass (1061.9 Da) matches a predicted phosphorylated peptide (1062.4 Da) corresponding to residues 510-520 (GSFGGGGSSDR) with one phosphated site.

(8). Analysis of phosphorylated peptide: YPpSLGpTGGGFR

In the same mass ion spectrum shown in Figure 3-13A the peak ion at m/z1271.3 present at 32.8 % of the most abundant peptide corresponds to the predicted phosphorylated peptide with charge +1 at m/z 1271.6. The observed mass of 1270.3 Da could be assigned to predicted phosphorylated peptide residues 199-209 (YPpSLGpTGGGFR) with two phosphorylation sites (theoretical 1110.6+160=1270.6 Da). The unphosphorylated peptide (theoretical 1110.6 Da) was not observed because the peptide can't be retained on IMAC column. Another form of this phosphorylated peptide was observed in the same figure 3-14A. The peptide ion at m/z 1173.4 corresponds to a Neutral loss of 98 Da from the predicted peptide ion with two phosphorylated sites [theoretical 1111.6 (MH^+) +160-98=1173.6].

(9). Analysis of phosphorylated peptide: EVpSEK

The mass ion spectrum shown in Figure 3-15A resulted from fraction 5^{th} tube of IMAC run. The peak at m/z 671.3 is in excellent agreement with the predicted residues 428-432 (EVpSEK) with one phosphorylated site (theoretical 591.3+80=671.3). It is possible that Ser^{430} was phosphorylated due to only one potential phosphorylated site.

(10). Analysis of phosphorylated peptide: AVNRPEpSEEEK

Reproduced with permission of the copyright owner. Further reproduction prohibited without permission.

The mass ion spectrum shown in Figure 3-16A and Figure 3-17A resulted respectively from total mixture peptides of different IMAC run. In Figure 3-16A the peak ion at m/z 1367.7 present at 10.6% of the most abundant peptide corresponds to the predicted phosphorylated peptide 389-399 (AVNRPEp**S**EEEK) with charge +1 at m/z 1367.6. In Figure 3-17A the peak ion at m/z 684.6 present at 2.9% of the most abundant peptide corresponds to the same predicted phosphorylated peptide with charge +2 at m/z 684.3. The observed mass of 1366.7 Da from m/z 1367.7 and 1367.2 Da from m/z 684.6 matched respectively with the predicted mass of 1366.6 Da for phosphorylated peptide 389-399 (AVNRPEp**S**EEEK) plus an additional 80 mass units due to the phosphate ester group. The unphosphorylated peptide ions (M=1286.8 Da) with charge +1 at m/z 1287.7 (Figure 3-16A-expansion), +2 at m/z 646.3 and +3 at m/z 429.9 were transferred to deconvolution mass spectrum obtained the molecular weight of 1286.8 Da (theoretical 1286.6 Da) because of the peptide contains four glutamic acid residues, which probably interacted with the iron on the IMAC column (19).

(11). Analysis of phosphorylated peptide: EIEAIAGDGpSEQAK

The mass ion spectrum shown in Figure 3-18A resulted from total mixture peptides of IMAC run. The peptides ion at m/z 1497.5 present at 33.5 % of the most abundant peptide corresponds to the predicted phosphorylated peptide with charge +1 at m/z 1497.7. The observed mass of 1496.5 Da matches the predicted mass (1496.7 Da) corresponding to peptide 414-427 (EIEAIAGDG<u>S</u>EQAK) with an additional 80 mass unites. A neutral loss of 98 Da from 1497.5 Da, eluting from next HPLC fraction, was observed at m/z 1399.6 with relative abundance of ~21.0% (theoretical 1497.7+80-98=1399.7) shown in mass ion spectrum in Figure 3-20A. The Ser^{423} is possibly

Reproduced with permission of the copyright owner. Further reproduction prohibited without permission.

phosphorylated due to only one serine and no threonine residue. An observed unphosphorylated peptide (1417.0 Da) appeared in the deconvolution mass spectrum shown in Figure 3-19A and 19B.

(12). Analysis of phosphorylated peptide: SDDIDNWSR

The mass ion spectrum shown in Figure 3-20A resulted from total mixture peptides of IMAC run. The peptide ion at m/z 1187.3 present at 26.0 % of the most abundant peptide corresponds to the predicted phosphopeptide peptide with charge +1 at m/z 1187.5. The observed mass of 1186.3 Da matches the predicted mass (1186.5 Da) of the phosphorylated peptide 182-190 (SDDIDNWSR) with an increase of 80 mass units. This peptide contains two potentially phosphorylated sites, thus one phosphate can't be assigned to exact site. It is possible that Ser^{182} was the phosphorylated.residue, because the presence of multiple acidic residues on the COOH- terminal side of the phosphorylation site in proteins and in peptides appears to be strongly preferred to the substrate recognition and phosphorylation by casein kinase II (46, 47 and 48). An observed peptide ion at m/z 1106.9 appeared in the mass ion spectrum could be assigned to a predicted unphosphorylated peptide with +1 charge at m/z 1107.5. It is possible to appear due to three aspartic acid residues (data not shown).

(13) Analysis of phosphorylated peptide: SSR

The sample resulted from total mixture peptides of IMAC run. The mass ion spectrum in Figure 3-21A and expanded Figure 3-21A elute from HPLC fraction. The peptide ion at m/z 331.3 is in excellent agreement with a neutral loss of 98 Da from the predicted peptide ion 136-138 (SSR) containing one phosphorylated site with +1 charge at m/z 331.2 (theoretical 349.2+80-98=331.2). The peptide ion at m/z 313.3 is also in excellent

Reproduced with permission of the copyright owner. Further reproduction prohibited without permission.

agreement with neutral loss of two H_3PO_4 (196 Da) from predicted peptide ion 136-138 (SSR) containing two phosphorylated sites with +1 change at m/z 313.2 (theoretical 349.2+160-196=313.2) but this ion with low relative abundance also appeared in mass ion spectrum of background from non-phosphorylated eIF4B protein digest without IMAC run. Any peptide happens to have the same m/z value as the putative phosphopeptide and therefore this putative peptide is not considered to be possible phosphopeptide. The phosphorylated peptide (SSR) was possibly modified at lest one serine, and further confirmation from tandem mass spectrometry is needed.

(14). Analysis of phosphorylated peptides: ADESDNWGK or FGQRPSSGAGR

Negative-ion ESI mass spectrum shown in Figure 3-22A and 22B were performed using aqueous solution of pH 6.5 due to 4B peptides occur dephosphorylation in basic condition (3). The Figure 3-22A demonstrated $[M-H]^-$ ion at m/z 1099.5 and $[M-2H]^{2-}$ ion at m/z 549.4, and gave an average mass of 1100.5 in deconvolution mass spectrum (Figure 3-22B). The observed mass of 1100.5 corresponds to two possible phosphorylated peptides, one is residues 148-156 (ADESDNWGK) with one phosphorylated site (theoretical 1020.4+80=1100.4 Da) and another one is residues 453-463 (FGQRPSSGAGR) with a neutral loss of 98 Da (theoretical 1118.6-98=1100.6 Da), so we could not identify which is the exact phosphorylated peptide based on the mass of 1100.5 Da although the residues ADESDNWGK appears to be preferred to phosphorylate by casein kinase II. Further confirmation from tandem mass spectrometry will be needed to remove any ambiguity in peptide assignment by sequencing. The unphosphorylated peptide (theoretical 1020.4 Da) did not appear in negative mass spectrum.

Reproduced with permission of the copyright owner. Further reproduction prohibited without permission.

3.) Summary

As a result of mass spectral analysis, thirteen phosphorylated peptides could be identified. Six phosphorylated peptides were shown respectively in both mass ion spectra and devolution mass spectra in positive mode. Ten sites in five phosphorylated peptides can be assigned the exact phosphorylated locations due to the observed phosphorylation site match with the potential phosphorylation site in each peptide shown in Table 3-1. Seven possible phosphorylated peptides were shown in mass ion spectra but did not appear in devolution mass spectra because the ions did not have multiple charged states, only single charge state or lower amplitude. It has been suggested that protonation occurs at basic residues (Arg, Lys, His, NH_2-terminus) for positive ion spectra. The maximum number of charges is consistent with the number of basic residues (positive ion ESI) for smaller proteins and peptides (49, 50, 51). Since trypsin specifically cleaves peptide bonds C-terminally at lysine and arginine, not before proline. The resulting peptides will tend to form singly charged as well as doubly charged molecular ions except residues 284-295, 389-399, where lysine and arginine were followed by a proline residue. The two peptides each have two basic residues (RPSPFGAAKPR and AVNRPESEEEK) and one additional NH_2-terminus. Two charges are generally expected to reside on opposite ends of the molecule due to an arginine or lysine residue at the C-terminus and the N-terminus basic site (49, 50). For smaller phosphorylated peptides containing only one basic residue, the maximum number of positive charge is +2. Unsurprisingly, these peptides produced only singly charged fragment ion $[M+H]^+$. This may be because phosphorylation of a protein at an individual site can often be quite low. The assignment of phosphorylated peptide ion was determined by the following: First, the phosphorylated

Reproduced with permission of the copyright owner. Further reproduction prohibited without permission.

peptide ion was detected by an increase of 80 Da (or multiples of 80 Da) of predicted peptide ion or by loss of 98 Da (or multiples of 98 Da) of predicted phosphorylated peptide ion. Second, these ions resulted from purified phosphorylated eIF4B protein digest after IMAC run and they were not observed from the ESI/MS spectra of non-phosphorylated eIF4B protein digest without IMAC run. This may be explained that these ions did not come from background ions containing non-phosphorylated peptides and peptides formed by autolysis of trypsin. The possible phosphorylated peptides were shown in Table 3-2. Seven residues underlined were possible phosphorylated sites due to all the potential phosphorylation site(s) in each peptide were phosphorylated. Further confirmation could be done by tandem mass spectrometry if it is necessary.

Two dominant phosphorylation regions underlined in eIF4B sequence are observed. One appears in residue regions 136-204 on the NH_2-terminal side and another residue region 395-444 on the COOH-terminal side (see sequence of eIF4B). The confirmed phosphorylated sites are indicted by labeled (•) on the top. The possibly phosphorylated sites are indicted by labeled (−) on the top. The peptide under bold line is indicted that only one of two serines is phosphorylated. The peptide under two lines is indicted that only two of three serines are phosphorylated

MAKPWGGVGA WALDAEREDE EREHAAAFPA PDPPAAAGGA ASFPSLKEAV VAGGGKQKKK
KGTTLSLSEF TTYGAAGAPR RVAPAEPKGL TPQEMMMLPT GPRERSEDEL DRSRGFRSYG
GDREPRGGGF DDDRRSSRDS DLDMPSRADE SDNWGKNKSP SPAPTDSGRR DRLSGPSPLG
RSDDIDNWSR DKKPLPSRYP SLGTGGGFRE SSGGGPRESS GGGPRESSGG GFRDSPGPSD
SDRWVRGAVP APHTNNGDRP RLNLNPPKRD PSATPVPAAE VARSRPSPFG AAKPREEVLA
EKGLDWRKME GEIEKKTSRP TSSHSSRPNS AHSSRPGSPG SQVSAVGSEG APRARPKVNP
PGDAKPREVV LQEKGKDWRK IDLELEHRAV NRPESEEEKN LKEEINLLKV DLKEIEAIAG
DGSEQAKEVS EKISQMEKQL DLLTVELDDK IRFGQRPSSG AGRAAAPPPA SEEPHVAVAH
MDRPRSRGGV ETYPKPVEER WGPHGSRERG SFGGGGSSDR SSTRQGW

Reproduced with permission of the copyright owner. Further reproduction prohibited without permission.

Conclusions

In this study, we report a powerful technique for isolation of phosphorylated peptides using affinity-bound to Fe (III)-IMAC column with buffer (0.1% NH_4Ac, 2 mM $(NH_4)H_2PO_4$ pH 8.0) and direct HPLC-ESI/MS analysis of phosphorylated peptides without any additional desalting step when a Agilent 1100 LC/MSD instrument was used. HPLC-ESI/MS was used to analyze phosphorylated peptides from purified eIF4B protein without the necessity of radiolabeling the protein. The phosphorylated peptides with known sequence were identified by detection of 80 Da mass increments. We provide evidence that ESI/MS also can lose the elements of H_3PO_4 during collision activation, resulting in a neutral loss of 98 Da (or a multiple of 98 Da) with a more efficient peak than that with increase of 80 Da. This may be explained as a negative charge is converted to a neutral group, reducing the suppression effects for phosphopeptides in positive mode ionization. This β-eliminated phosphopeptides produce characteristic signatures and provide unambiguous evidence for phosphopeptides by ESI-MS. This is similar to matrix-assisted laser desorption/ionization (MALDI) ion trap mass spectrometry and ESI-tandem mass spectrometry (ESI-MS/MS). This approach may have broader application for assays monitoring *in vitro* phosphorylation events.

So far, twenty-one phosphorylation sites have been observed from a total of 59 serine and 15 threonine residues. Ten phosphorylated sites can be confirmed after deconvolution. Seven phosphorylated sites can be possibly determined in ion mass spectra because their peptide ions were not transferred into deconlovolution mass spectra. Their sites can be determined because all the serine and / or threonine residues were phosphorylated in each peptide. Another four sites in three peptides can not be uniquely

Reproduced with permission of the copyright owner. Further reproduction prohibited without permission.

identified by ESI/MS because each peptide contains more potential phosphorylation sites than observed phosphorylated site(s). The two dominant phosphorylation regions by the contribution of CKII correspond to NH_2-terminal residues 136-204 and COOH-terminal residues 395-444. We find that all the sites are not identically phosphorylated on a molecule of eIF4B and that six peptides 139-147, 159-169, 199-209, 414-427, 439-450, 510-520 in Table 3-1 and Table 3-2 exist in different forms, This may be one reason that eIF4B phosphoprotein appears as several isoelectric forms in two-dimensional isoelectric focusing (IEF)/SDS-PAGE (4).

Future studies will exploit the possibility that the two phosphorylated regions and specific sites may be used in investigating the functional significance of phosphorylation in eIF4B-eIF4F, eIF4B-peptide, eIF4B-DNA and eIF4B-mRNA interactions by modification via site- directed mutagenesis. ESI-MS has become an important tool for the study of non-covalent band complexs. The following tests may be proposed:

eIF4B peptide-mRNA interactions-------Phosphorylated eIF4B trypsin digest after Fe-IMAC contain phosphorylated peptides and peptides with a high level of acidic residues. They are mixed with mRNA under different pH value for ESI-MS analysis. A series of multiply changed ions with the charge distribution states will be shown in the ion mass spectra and the molecular masses of mRNA-bound species of eIF4B peptides will appear in deconvolution mass spectra. Phosphorylated peptides and unphosphorylated peptides binding to mRNA can be determined according to their masses. The phosphorylation sites involved can be identified. The same method could be used to determine which of phosphoylated peptides bind to DNA and other proteins (52).

Reproduced with permission of the copyright owner. Further reproduction prohibited without permission.

Wild-type eIF4B and mutation eIF4B -mRNA interactions------ Serine or threonine residues can be repleced with either alanine or glutamate mutations in mRNA-bound phosphorylation sites. A series of mutation eIF4B need to be set up, in which one or two serines are substituted with either alanine (to block phosphorylation) or glutamate (to mimic phosphorylation) and expressed in *E.coli*. The protein are mixed with mRNA respectively under different pH value and ESI-MS analysis compared with analysis of wild-type eIF4B-mRNA interactions. The phosphorylation sites that are functional important for binding mRNA can be identified.

Conformation of phosphorylated eIF4B and unphosphorylated eIF4B------ Testing of whether phosphorylation causes tertiary conformational changes may be determined by analysis of mass spectra between phosphorylated eIF4B and unphosphorylated eIF4B. ESI mass spectra of a protein show a series of multiply changed ions with the charge numbers reflecting the conformational states of protein. A broad charge distribution could shift between high and low m/z under the conditions of study, such as pH, temperature, and the presence of denaturing agents (52). In general, a tightly folded protein will have fewer basic sites available for protonation compared to the same unfolded protein. Charge distribution with a set of small numbers will come into higher m/z range, which corresponding to native state of protein. Charge distribution with a set of higher numbers will appear at lower m/z range, which corresponds to the denture state of protein. Generally, a set of charge distribution moving from high to low m/z corresponds to native state, partially unfolded state, unfolded state and destroyed state. Compared the charge distribution states in mass spectra we can know whether

Reproduced with permission of the copyright owner. Further reproduction prohibited without permission.

phosphorylation sites can play an important rule in tertiary structure. Structural analysis for eIF4B binding to mRNA may be possible using the same method.

Reproduced with permission of the copyright owner. Further reproduction prohibited without permission.

Table 1-1. Restriction analysis of eIF4B plasmid DNA

Reproduced with permission of the copyright owner. Further reproduction prohibited without permission.

Table 1-1

Prototype enzyme	Recognition Sequence	Restriction # Sites	Fragment weight
BamH I	GGATCC	1	4637 + 1679 = 6317bp
BamH I XbaI	GGATCC TCTAGA	2	1679 + 78 = 1757bp 6317 – 1757 = 4560bp
HindIII XbaI	AAGCTT TCTAGA	2	1679 + 559 = 2238bp 6317 – 2238 = 4079bp

Reproduced with permission of the copyright owner. Further reproduction prohibited without permission.

Figure 1-1. Restriction analysis of eIF4B plasmid DNA Lane 1, the DNA ladder; Lane 2, double digests with Hind III and Xba I, the sample was not completely digested, the top band corresponded to molecular weight of intact eIF-4B Plasmid (6317) and is consistent with the highest band of a control eIF-4B Plasmid. The other two bands corresponded to molecular weights of fragments of eIF-4B Plasmids (2238, 4079). Lane 3, sample was almost completely digested by BamH I and Xba I, and two bands correspond to molecular weights of fragments of eIF-4B Plasmids (4560, 1759). Lane 4, a sample provided by Dr. K. Browning, U. of TX, used as a control was almost completely digested by BamH I and Xba I, and the molecular weights of two fragments were consistent with sample 3.

Reproduced with permission of the copyright owner. Further reproduction prohibited without permission.

Figure 1-1

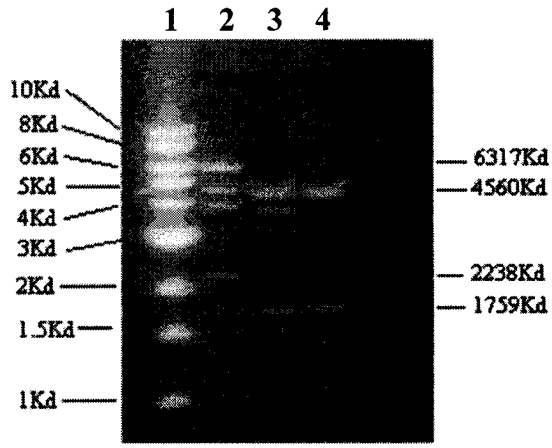

Reproduced with permission of the copyright owner. Further reproduction prohibited without permission.

Figure 1- 2. HiTrap SP column and P60 chromatography of eIF-4B protein. (A) The partially purified eIF4B protein fractions from HiTrap SP column were pooled, and rerun on a HiTrap SP column. (B) The fractions 18,19 and 20 were pooled and concentrated, and loaded on Bio-Gel-P-60 column. The eIF4B protein was eluted with buffer (10mM Tris.,10mM KCl). The samples of fractions were analyzed by gel electrophoresis on a 10% SDS-PAGE and visualized by staining with Coomassie Blue. Molecular size markers were shown on the left. (C) Crude supernatant of original eIF4B sample.

Reproduced with permission of the copyright owner. Further reproduction prohibited without permission.

Figure 1-2

Fractions of purification of 4B protein

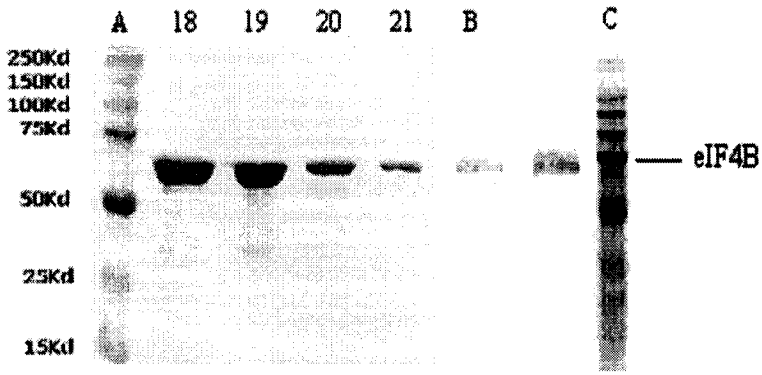

Reproduced with permission of the copyright owner. Further reproduction prohibited without permission.

Figure1-3. Immunoblots of eIF-4B. Lane 1, putative purified protein; Lane 2, cellular extracts from nonexpressing cells; Lane 3, cellular extract from eIF-4B expressing cells. The indicated proteins were loaded on an SDS-PAGE (10%) and transferred to nitrocellulose. The blot was probed with a 1: 500 dilution of the recombinant eIF4B antibody (Karen S. Browning's Lab), followed by a 1:1000 dilution of anti-rabbit lgG HRP (Promega). Color was developed with 15 ml of 4-chloro-1-naphthol (SIGMA) with 60 ul of 3% H_2O_2 (SIGMA).

Reproduced with permission of the copyright owner. Further reproduction prohibited without permission.

Figure 1-3

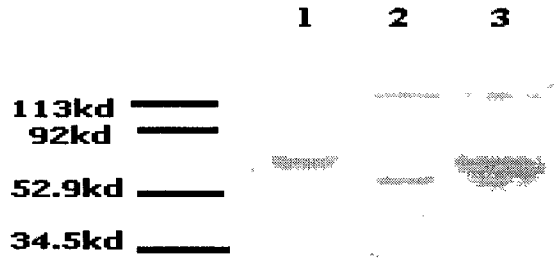

Reproduced with permission of the copyright owner. Further reproduction prohibited without permission.

Figure 2-1. Phosphorylation and dephosphorylation of protein

Reproduced with permission of the copyright owner. Further reproduction prohibited without permission.

Figure 2-1.

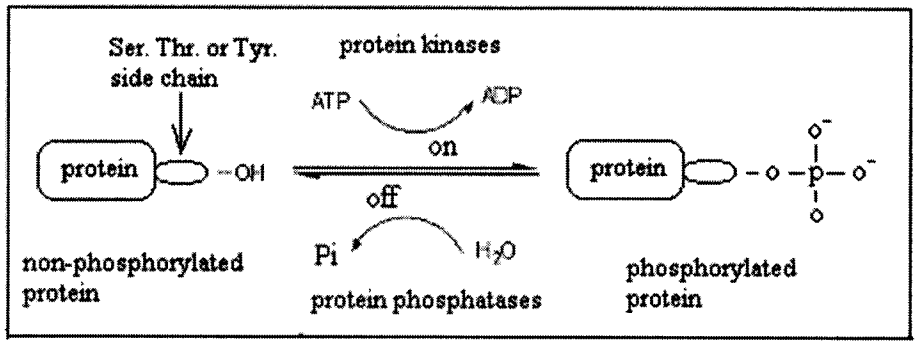

Reproduced with permission of the copyright owner. Further reproduction prohibited without permission.

Figure 2-2. Comparison between unphosphoprotein and phosphoprotein of eIF4B

Lane 1, 2 ul of 2.2 ug eIF4B, 15 ul of CKII buffer (20 mM tris·HCl, 50 mM KCl, 10 mM $MgCl_2$, pH 7.3);

Lane 2, 2 ul of 2.2 ug eIF4B, 15 ul of CKII buffer and 1 ul of 33.0 U CKII;

Lane 3, 2 ul of 2.2 ug eIF4B, 15 ul of CKII buffer, 1 ul of 33.0 U CKII and 2 ul of 10 mM ATP;

Then added dH_2O to a final volume of 20 ul

Three samples were incubated at 30.5 ^0C for 2 hours, and were electrophoresed on a 10% SDS-PAGE gel for 3 hours and were visualized by staining with Coomassie Blue.

Reproduced with permission of the copyright owner. Further reproduction prohibited without permission.

Figure 2-2

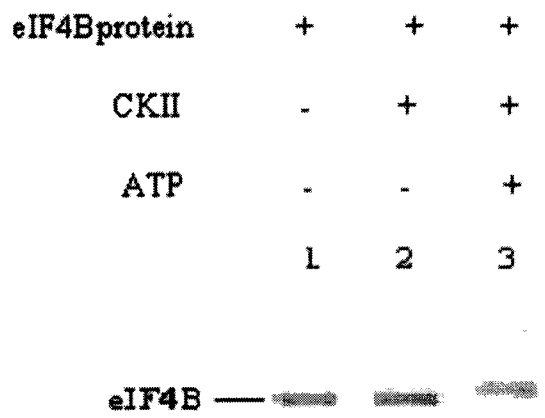

Reproduced with permission of the copyright owner. Further reproduction prohibited without permission.

Figure 2-3. Enrichment of phosphorylated peptides of eIF4B protein by Fe (III)-IMAC. The phosphorylated eIF4B protein trypsin digest was loaded onto the Fe (III)-IMAC column at a pH of 3.3 and increasing the pH of the buffer to 8.0 eluted the retained components. Peak 1 is due to unretained components and peak 2 is due to retained components.

Reproduced with permission of the copyright owner. Further reproduction prohibited without permission.

Figure 2-3

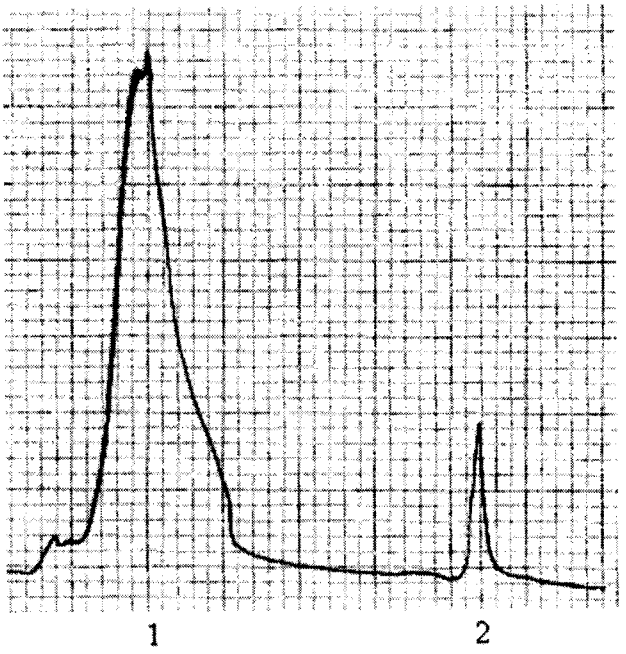

Reproduced with permission of the copyright owner. Further reproduction prohibited without permission.

Figure 3-1. Schematic diagram for mass spectrometry with an electrospray ion Source The essential features of ESI Mass Spectrometer include the five same basic parts as any mass spectrometer: a sample introduction device, an ionization source, a vacuum system, a mass analyzer and an ion detector.

Reproduced with permission of the copyright owner. Further reproduction prohibited without permission.

Figure 3-1.

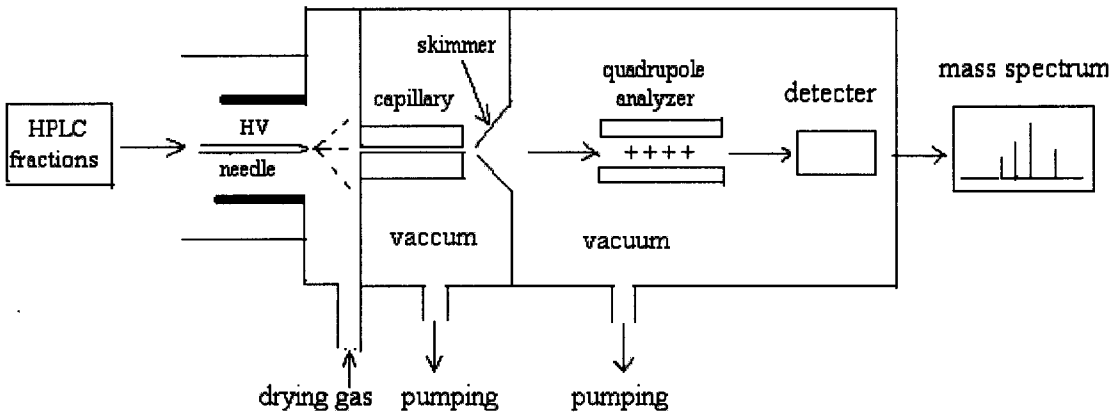

Reproduced with permission of the copyright owner. Further reproduction prohibited without permission.

Table 3-1. Phosphorylated peptides and sites of eIF4B confirmed in the deconvolution mass spectra

a. All M values are isotope-averaged. Oberved M is the deconvoluted phosphopeptide mass.

b. Calculated mass is from theoretical isotope-averaged mass of peptide sequence with the addition of 80 Da (or a multiple of 80Da) and / or loss of 98Da (or a multiple of 98Da)

All masses are expressed in Daltons The identified phosphorylated residues are boldface.

c. (Q→E) indicated that the glutamine was converted to glutamic acid by deamidation.

A sign (*) indicated that the phosphorylated peptide existed two forms. One form (1279.8) corresponded to mass increase of 2x80 Da with two phosphate groups. Another form (1048.2)) corresponded to a loss of 4x98 Da from four phosphorylated serine residues.

Underlined residues 139-147 and 439-450[c] also appeared in Table 3-2

Reproduced with permission of the copyright owner. Further reproduction prohibited without permission.

Table 3-1.

Residue no.	peptide sequence	observed M[a]	calculated M[b]	site no
139-147	DSDLDMPSR	1016.5	1016.4	1
159-169*	SFSPAPTDSGR	1279.8 1048.2	1280.5 1048.5	2 4
173-181	LSGPSPLGR	1043.2	1043.5	2
284-295	SRPSPFGAAKPR	1332.0	1331.7	2
433-436	ISQMEK	814.4	814.4	1
433-436[c]	IS (Q→E) MEK	815.5	815.5	1
439-450[c]	(Q→E) LDLLTVELDDK	1383.6	1383.7	1

Reproduced with permission of the copyright owner. Further reproduction prohibited without permission.

Table 3-2. Phosphorylated peptides and sites of eIF4B possibly identified in the ion mass spectra

a. Only a singly charged species were detected, so observed masses of phosphorylated peptides were done manually.

b. Calculated mass is from theoretical isotope-averaged mass of peptide sequence with the addition of 80 Da (or a multiple of 80Da) and / or loss of 98Da (or a multiple of 98Da)

All masses are expressed in Daltons. The residues underlined are possibly phosphorylated sites.

Signs (* [a], * [b], * [c], and * [d]) indicated that the four phosphorylated peptides exited two forms respectively. Signs (* [a]) indicated that one form (1194.7) corresponded to increase of 2x80 Da. Another form (1097.0)) corresponded to a loss of 98 Da from previous form. Signs (* [b]) indicated that one form (1270.3) corresponded to increase of 2x80 Da. Another form (1173.4) corresponded to a loss of 98 Da from previous form. Signs (* [c]) indicated that one form (1497.5) corresponded to increase of 80 Da. Another form (1399.6) corresponded to a loss of 98 Da from previous form. Signs (* [a]) indicated that one form (1143.0) corresponded to increase of 2x80 Da. Another form (1061.9) corresponded to a loss of 98 Da from previous form.

Underlined residues 139-147* [a] and 439-450 also appeared in Table 3-1

Reproduced with permission of the copyright owner. Further reproduction prohibited without permission.

Table 3-2.

Residue no.	peptide sequence	observed M[a]	calculated M[b]	site no
136-138	SSR	331.3	331.2	1
139-147* [a]	DSDLDMPSR	1194.7	1194.4	2
		1097.0	1096.4	2
182-190	SDDIDNWSR	1186.3	1186.5	1
199-209* [b]	YPSLGTGGGFR	1270.3	1270.6	2
		1173.4	1173.6	2
389-399	AVNRPESEEEK	1366.7	1366.6	1
414-427* [c]	EIEAIAGDGSEQAK	1497.5	1497.7	1
		1399.6	1399.7	1
428-432	EVSEK	670.3	670.3	1
439-450	Q LDLLTVELDDK	1480.6	1480.7	1
510-520* [d]	GSFGGGGSSDR	1143.0	1143.4	2
		1061.9	1062.4	1

Reproduced with permission of the copyright owner. Further reproduction prohibited without permission.

Figure 3-2A and 2B. Analysis of phosphorylated peptide IpSQMEK

This peptide from HPLC-ESI/MS analysis was shown in Figure 3-2A and 2B. The observed mass of 814.4 Da with relative abundance 15.56 of the largest signal peak in deconvolution mass spectrum is in excellent agreement with residues 433-436 (IpSQMEK) with one phosphorylated site at Ser^{434} (theoretical 734.4+80 = 814.4 Da) due to only one potential phosphorylation site in this peptide.

Reproduced with permission of the copyright owner. Further reproduction prohibited without permission.

Figure 3 – 2A

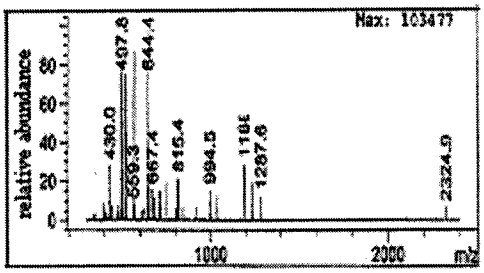

Figure 3 – 2B

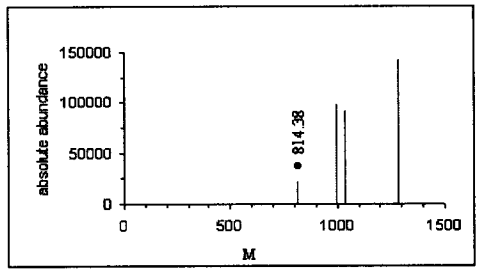

Reproduced with permission of the copyright owner. Further reproduction prohibited without permission.

Figure 3-3A and 3B. Analysis of phosphorylated peptide: pSRPpSPFGAAKPR

The peptide ions with single, double and triple charges ([MH^+ = 1332.7, $[M + 2H]^{2+}$ = 666.9 and $[M + 3H]^{3+}$ = 445.0]) were detected in Figure 3-3A and displayed mass of 1332.0 Da in Figure 3-3B after deconvolution. This peptide resulted from a prominent neutral loss of phosphoric acid (98 Da) from residues 284-295 pSRPpSPFGAAKPR with two phosphorylated sites (theoretical 1269.7 + 160 – 98 = 1331.7 Da). The presence of phosphate groups on this peptide was confirmed at Ser^{284} and Ser^{287} due to only two serine residues in the peptide.

Reproduced with permission of the copyright owner. Further reproduction prohibited without permission.

Figure 3 – 3A

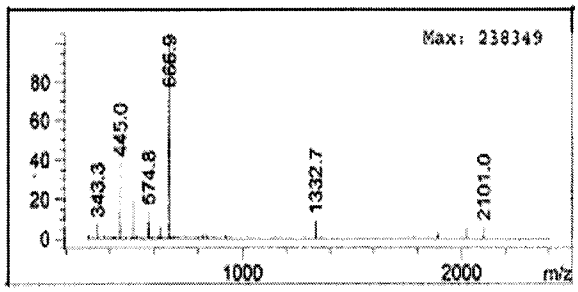

Figure 3 – 3B

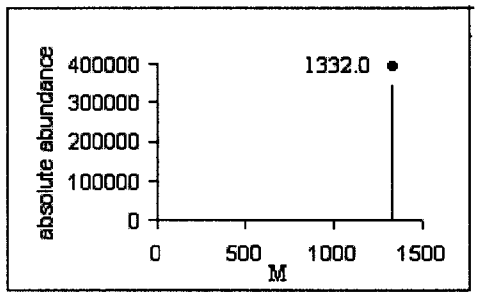

Reproduced with permission of the copyright owner. Further reproduction prohibited without permission.

Figure 3-4A and 4B. Analysis of phosphorylated peptide: SFSPAPTDSGR

The mass ion spectrum in Figure 3-4A yields the deconvolution mass spectrum shown in Figure 3-4B. The peak at 1279.8 Da with absolute abundance of 36385 was mass 160 Da higher than the calculated mass of residues 159-169 (SFSPAPTDSGR) (theoretical 1120.5 + 160 = 1280.5 Da) . Three serine residues and one threonine residue are contained within the peptide, thus the two sites of phosphorylation cannot be assigned based on the molecular mass data.

Reproduced with permission of the copyright owner. Further reproduction prohibited without permission.

Figure 3 – 4A

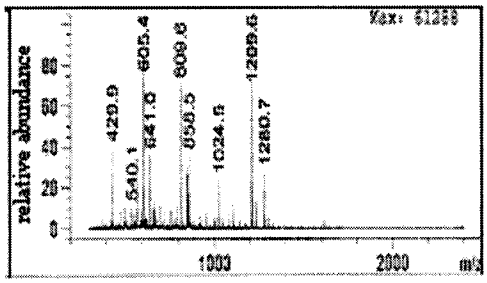

Figure 3 – 4B

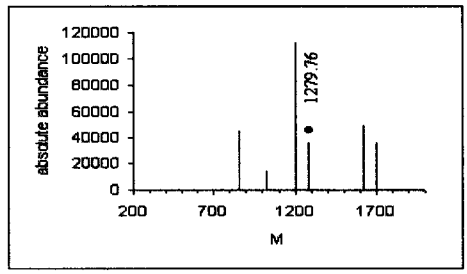

Reproduced with permission of the copyright owner. Further reproduction prohibited without permission.

Figure 3-5A and 5B. Analysis of another form of phosphorylated peptide: pSFpSPAPpTDpSGR.

It was observed that this peptide was present in another form and eluted in a later HPLC fraction. The mass spectra were shown in Figure 3-5A and 5B. The peak at 1048.2 Da in Figure 3-5B with lower absolute abundance of 9444 corresponds to the predicted residues 159-169 with neutral loss of 4x98 Da (theoretical 1120.5-4x8 = 1048.5 Da). This may be explained that four potential phosphorylation sites of a small amount of the peptides have chance to obtain phosphate groups at Ser^{159}, Ser^{161}, Thr^{165} and Ser^{167} but most of phosphorylated peptide contains only two phosphorylated sites.

Analysis of phosphorylated peptide: LpSGPpSPLGR

The peak at 1043.2 Da in Figure 3-5B was present with absolute abundance of 8815 corresponds to the predicted phosphorylated residues 173-181 (Lp**S**GPp**S**PLGR) containing two phosphorylated sites at Ser^{174} and Ser^{177} (theoretical 883.5+160 = 1043.5 Da).

Reproduced with permission of the copyright owner. Further reproduction prohibited without permission.

Figure 3 – 5A

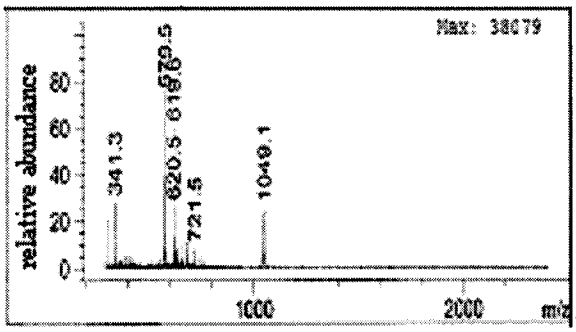

Figure 3 – 5B

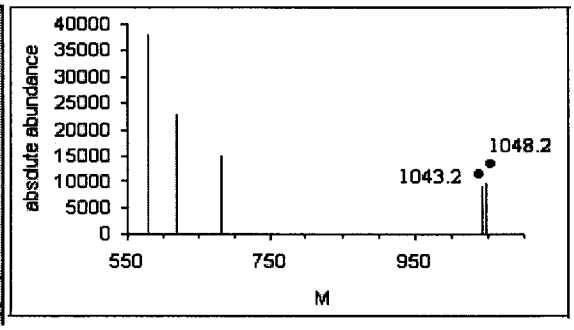

Reproduced with permission of the copyright owner. Further reproduction prohibited without permission.

Figure 3-6A and 6B. unphosphorylated peptide: QLDLLTVELDDK

An observed unphosphorylated peptide with multiply charged states and mass of 1401.1 Da appeared respectively in Figure 3-6A and 6B. Both three Asp recidues and one Glu residue have affinity for the Fe (III)-IMAC (19).

Reproduced with permission of the copyright owner. Further reproduction prohibited without permission.

Figure 3-6A

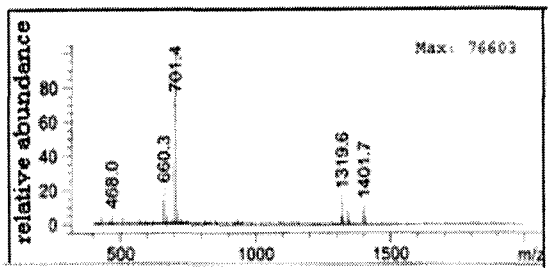

Figure 3-6B

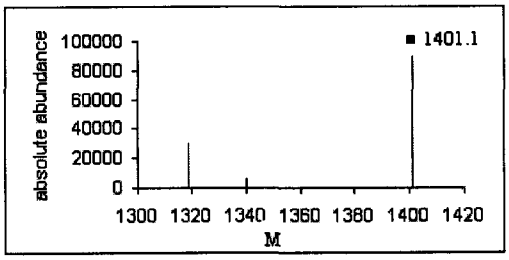

Reproduced with permission of the copyright owner. Further reproduction prohibited without permission.

Figure 3-7A and 7B. Analysis of phosphorylated peptide: (Q→E)LDLLpTVELDDK

The sample from total mixture peptides of another IMAC run was analyzed by HPLC-ESI/MS. The multiply charged state of mass ion spectrum shown in Figure 3-7A was transferred to deconvolution mass spectrum shown in Figure 3-7B. The peak at 1383.6 Da corresponds to a prominent neutral loss of 98 Da with absolute abundance of 124954 from the predicted residues 439-450, (Q→LDLLp**T**VELDDK) with only one phosphorylated site at Thr^{444} and deamidation of the glutamine to glutamic acid (theoretical 1400.7+1 + 80 – 98 = 1383.8 Da).

(Q→E) indicated the deamidation of the glutamine to glutamic acid

Reproduced with permission of the copyright owner. Further reproduction prohibited without permission.

Figure 3-7A

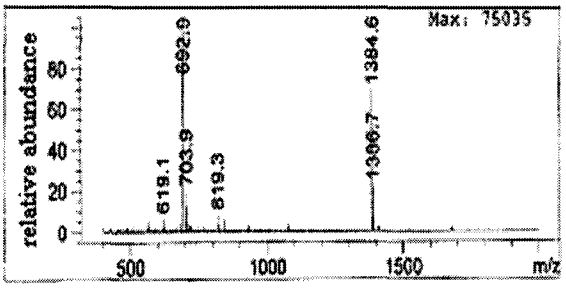

Figure 3-7B

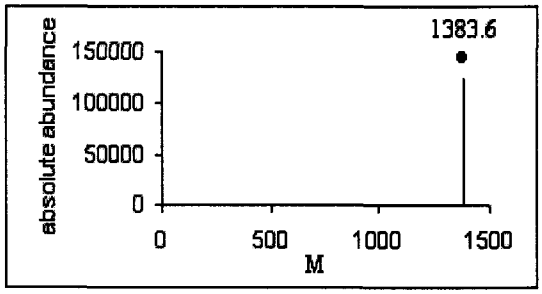

Reproduced with permission of the copyright owner. Further reproduction prohibited without permission.

Figure 3-8A. Analysis of phosphorylated peptide: QLDLLpTVELDDK

Another possible form of this peptide was found in fraction 7th tube of additional time IMAC run and was observed only in mass ion spectrum (Figure 3-8A). The peak ion at m/z 1481.6 present at 20.80% of the most abundant peptide is in good agreement with the predicted phosphorylated peptide with charge + 1 at m/z 1481.7. The ion was not observed in multiply charged states of mass ion spectra of unphosphorylated protein digest. The observed mass of 1480.6 Da matches with the predicted mass (1480.7 Da) corresponding to phosphorylated residues 439-450 (QLDLLpTVELDDK) at Thr^{444} due only one potential phosphorylated site. An observed unphosphorylated peptide ion (MH^+ = 1401.8) also appeared in the same mass ion spectrum.

Reproduced with permission of the copyright owner. Further reproduction prohibited without permission.

Figure 3-8A

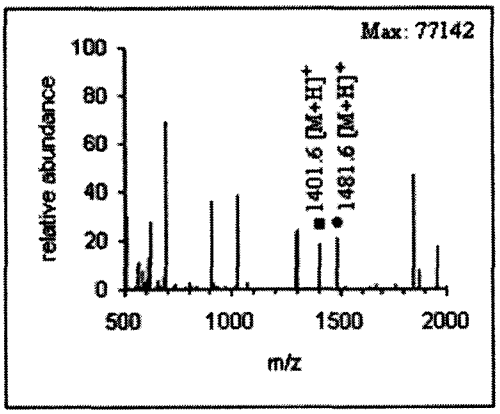

Reproduced with permission of the copyright owner. Further reproduction prohibited without permission.

Figure 3-9A and 9B. Analysis of phosphorylated peptide: DSDLDMPSR

The mass spectrum shown in Figure 3-9A, 9B results from analysis of fraction 8th tube of IMAC run. The peak at 1016.5 Da in deconvolution mass spectrum (Figure3-9B) corresponds to a neutral loss of 98 Da from the residues 139-147 (DSDLDMPSR) with one phosphorylated site (theoretical 1034.4 + 80 – 98 = 1016.4 Da). The exact phosphorylated site can't be assigned due to two potential phosphorylation sites.

Reproduced with permission of the copyright owner. Further reproduction prohibited without permission.

Figure 3-9A

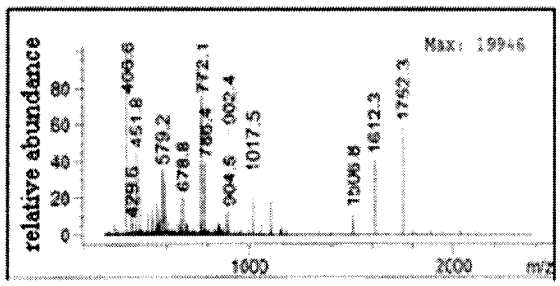

Figure 3-9B

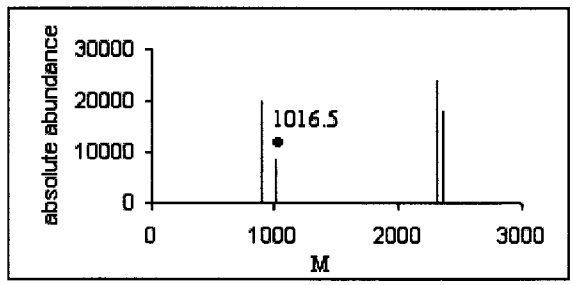

Reproduced with permission of the copyright owner. Further reproduction prohibited without permission.

Figure 3-10A. Analysis of phosphorylated peptide: DSDLDMPSR

This peptide was present in the other two forms, one with two phosphate groups existed in fraction 7th tube of IMAC run and shown in mass ion spectrum (Figure 3-10A). The peak at m/z 1195.7 with lower abundance could be assigned to the same residues 139-147 with two phosphorylated sites corresponding to predicted phosphorylated peptide ion (theoretical MH+ = 1035.4+160 = 1195.4). Another form was present in Figure 3-11A.

Reproduced with permission of the copyright owner. Further reproduction prohibited without permission.

Figure 3-10A

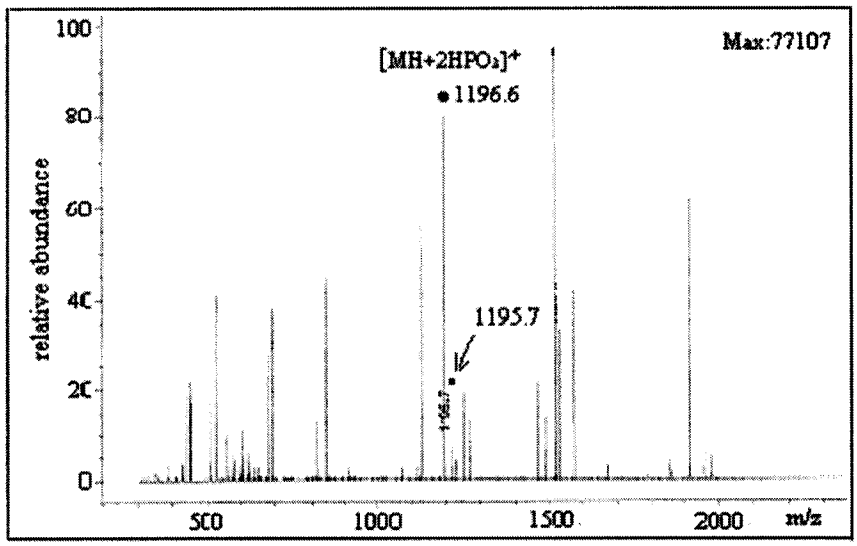

Reproduced with permission of the copyright owner. Further reproduction prohibited without permission.

Figure 3-11A. Another form of phosphorylated peptide: DSDLDMPSR

A prominent neutral loss of 98 Da from 1195.7 Da was observed in next eluting HPLC fraction.

Reproduced with permission of the copyright owner. Further reproduction prohibited without permission.

Figure 3-11A

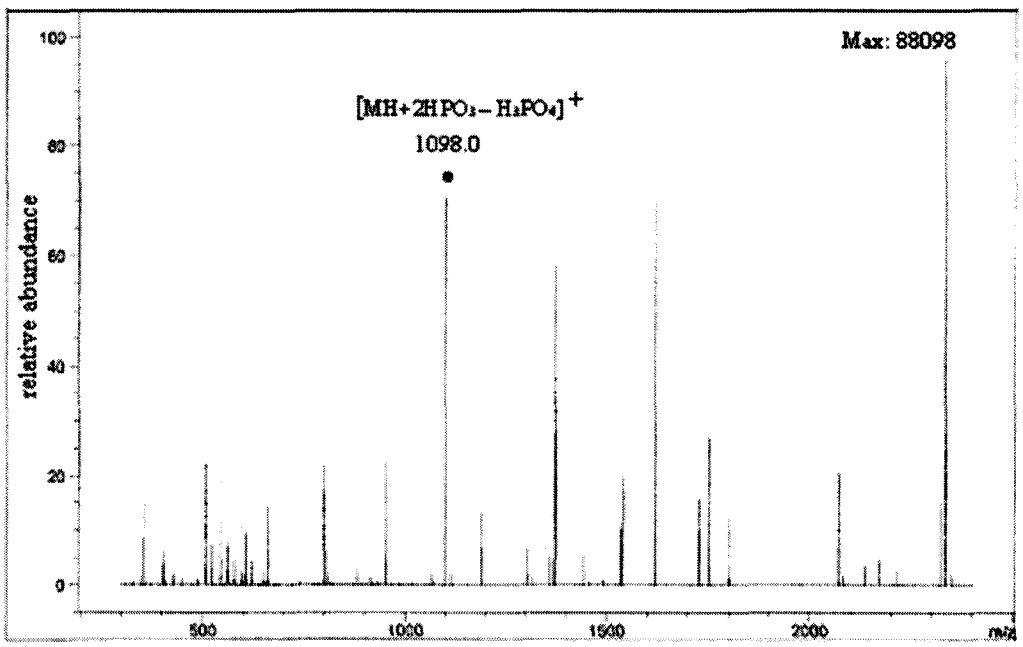

Reproduced with permission of the copyright owner. Further reproduction prohibited without permission.

Figure 3-12A and 12B. The unphosphorylated isotope peptide: DSDLDMPSR

The unphosphorylated peptide appeared in Figure 3-12B from HPLC-ESI/MS analysis. The unphosphorylated peptide ion appeared at m/z 1035.5 in Figure 3-12A corresponded to the phosphorylated ions at m/z 1195.7 with two phosphate groups.

Reproduced with permission of the copyright owner. Further reproduction prohibited without permission.

Figure 3-12A

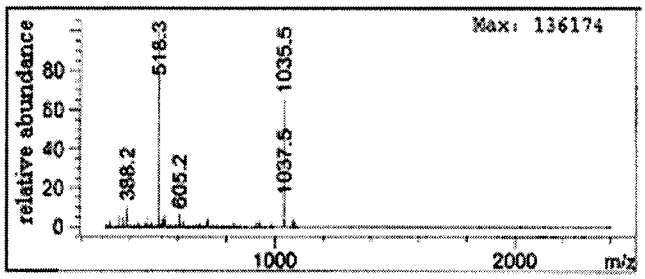

Figure 3-12B

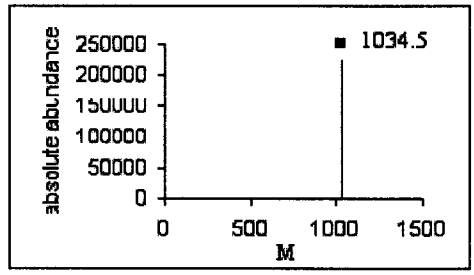

Reproduced with permission of the copyright owner. Further reproduction prohibited without permission.

Figure 3-13A. Analysis of phosphorylated peptide: GSFGGGGSSDR and YPSLGTGGGFR

The mass ion spectrum shown in Figure 3-13A resulted from fraction 7th tube of IMAC run. The ion at m/z 1143.0 present at 51.0% of the most abundant peptide corresponds to the predicted residues 510-520 (GSFGGGGSSDR) with two phosphorylated sites with charge +1 at m/z 1143.4 (theoretical 983.4+160=1143.4). The ion at m/z1271.3 present at 32.8 % of the most abundant peptide corresponds to the predicted phosphorylated peptide with charge +1 at m/z 1271.6. The observed mass of 1270.3 Da could be assigned to phosphorylated peptide residues 199-209 (YPSLGTGGGFR) with two phosphorylation sites (theoretical 1110.6+160=1270.6 Da).

Reproduced with permission of the copyright owner. Further reproduction prohibited without permission.

Figure 3-13A

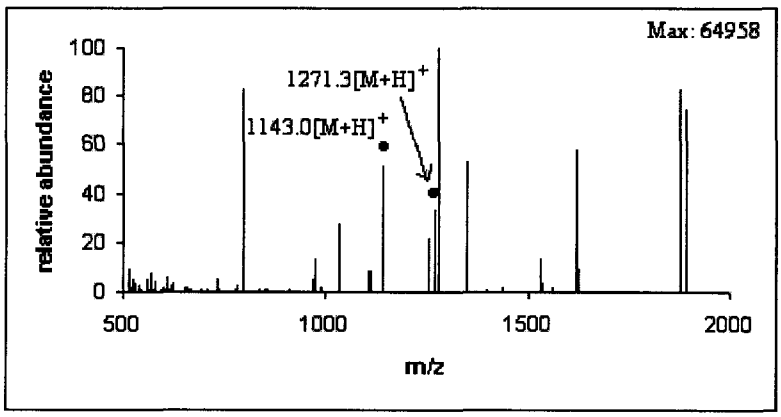

Reproduced with permission of the copyright owner. Further reproduction prohibited without permission.

Figure 3-14A. Another form of phosphorylated peptide: GSFGGGGSSDR and YPSLGTGGGFR

Sample resulted from total peptide mixture after IMAC run. The peptide ion at m/z 1062.9.0 was present at 7.8% of the most abundant peptide and the peak ion at m/z 531.9 (expanded Figure 3-14A) with 1.02% of the most abundant peptide correspond to the predicted phosphorylated peptide with charge +1 at m/z 1063.4 and with charge +2 at m/z 532.2, respectively. The observed average mass (1061.9 Da) matches another form predicted phosphorylated peptide GSFGGGGSSDR (1062.4 Da) with one phosphorylated site.

The peptide ion at m/z 1173.4 corresponds to a neutral loss of 98 Da from the predicted peptide ion with two phosphorylated sites (theoretical 1111.6+160-98=1173.6)

Reproduced with permission of the copyright owner. Further reproduction prohibited without permission.

Figure 3-14A

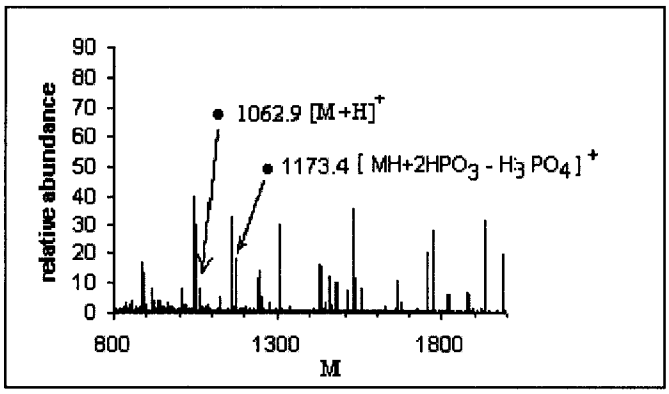

Reproduced with permission of the copyright owner. Further reproduction prohibited without permission.

Figure 3-14A-expanded

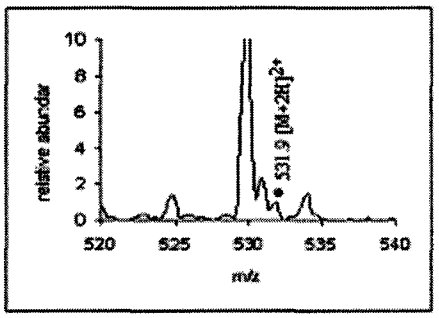

Reproduced with permission of the copyright owner. Further reproduction prohibited without permission.

Figure 3-15A. Analysis of phosphorylated peptide: EVpSEK

The mass ion spectrum shown in Figure 3-15A resulted from fraction 5th tube of IMAC run. The peak at m/z 671.3 is in excellent agreement with the predicated residues 428-432 (EVpSEK) containing one phosphorylated site with +1 charge at m/z 671.3 (theoretical 591.3+80=671.3). It is possible that Ser^{430} was phosphorylated due to only one potential phosphorylated site.

Reproduced with permission of the copyright owner. Further reproduction prohibited without permission.

Figure 3-15A

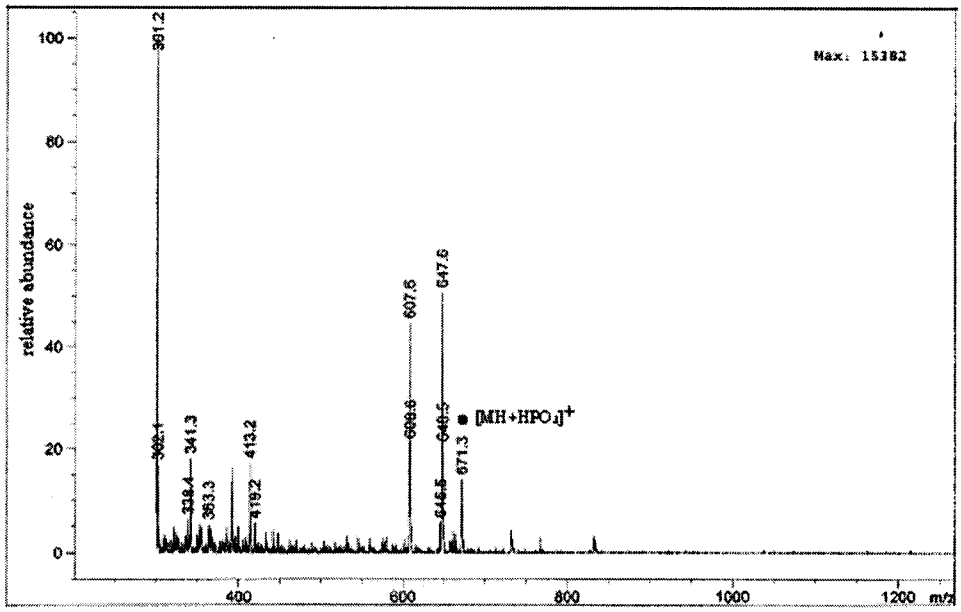

Reproduced with permission of the copyright owner. Further reproduction prohibited without permission.

Figure 3-16A and 16B. Analysis of phosphorylated peptide: AVNRPESEEEK

The mass ion spectrum shown in Figure 3-16A and Figure 3-17A resulted from total mixture peptides ofter IMAC run. In Figure 3-16A the peak ion at m/z 1367.7 present at 10.6% of the most abundant peptide is in excellent agreement with the predicted phosphorylated peptide 389-399 (AVNRPEpSEEEK) with charge +1 at m/z 1367.6. The observed mass of 1366.7 Da from m/z 1367.7 matched with the predicted mass of 1366.6 Da for phosphorylated peptide 389-399 (AVNRPEpSEEEK) plus an additional 80 mass units. The unphosphorylated peptide ions with charge +1 at m/z 1287.7 (Figure 3-15A-expansion), +2 at m/z 646.3 and +3 at m/z 429.9 in Figure 3-16A were transferred to deconvolution mass spectrum in Figure 3-16B and obtained the molecular weight of 1286.8 Da (theoretical 1286.6 Da) because of the peptide contains four glutamic acid residues, which probably interacted with the iron on the IMAC column (19).

Reproduced with permission of the copyright owner. Further reproduction prohibited without permission.

Figure 3-16A

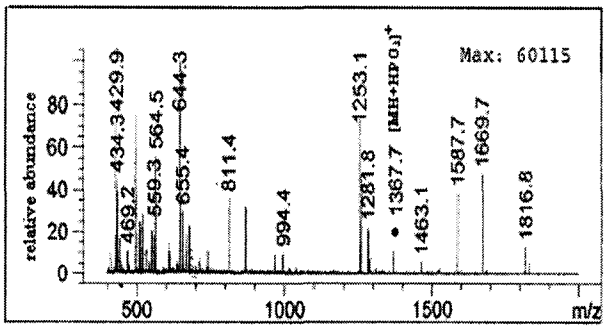

Figure 3-16B

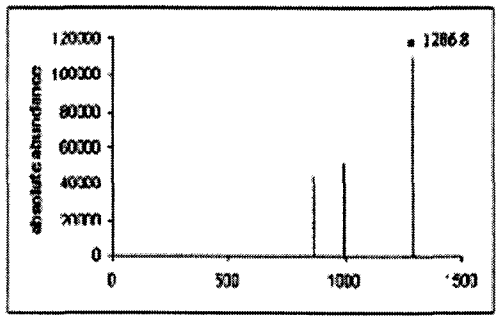

Reproduced with permission of the copyright owner. Further reproduction prohibited without permission.

Figure 3-16A-expansion

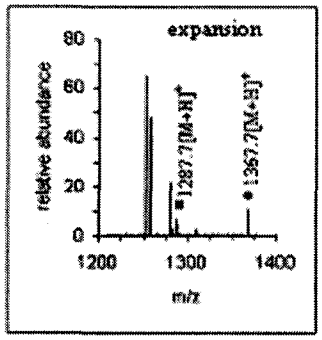

Reproduced with permission of the copyright owner. Further reproduction prohibited without permission.

Figure 3-17A. Analysis of phosphorylated peptide: AVNRPESEEEK

In Figure 3-17A the peak ion at m/z 684.6 present at 2.9% of the most abundant peptide corresponds to the same predicted phosphorylated peptide with charge +2 at m/z 684.3. The observed mass of 1367.2 Da from m/z 684.3 matched respectively with the predicted mass of 1366.6 Da for phosphorylated peptide 389-399 (AVNRPEpSEEEK) plus an additional 80 mass unites.

Reproduced with permission of the copyright owner. Further reproduction prohibited without permission.

Figure 3-17A

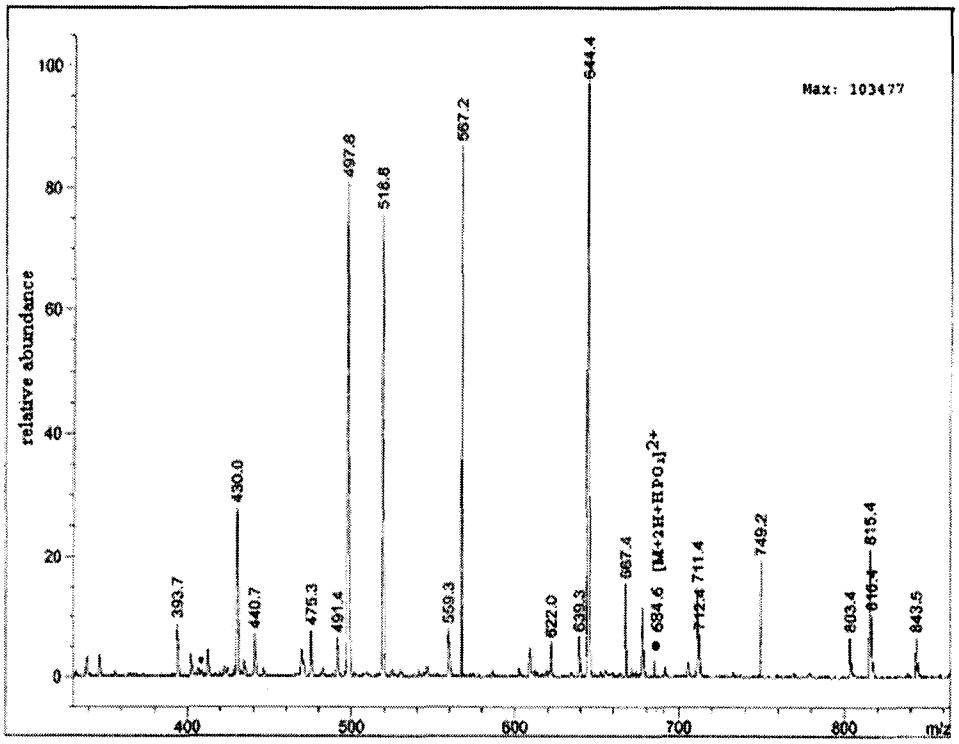

Reproduced with permission of the copyright owner. Further reproduction prohibited without permission.

Figure 3-18A. Analysis of phosphorylated peptide: EIEAIAGDGSEQAK

The mass ion spectrum shown in Figure 3-18A resulted from total mixture peptides of IMAC run. The peptides ion at m/z 1497.5 present at 33.5 % of the most abundant peptide corresponds to the predicted phosphorylated peptide with charge +1 at m/z 1497.7. The observed mass of 1496.5 Da matches the predicted mass (1496.7 Da) corresponding to peptide 414-427 (EIEAIAGDGSEQAK) with an additional 80Da. A neutral loss of 98 Da from next HPLC fraction, was observed at m/z 1399.6 with relative abundance of ~21.0% (theoretical 1497.7+80-98=1399.7) shown in Figure 3-20A The Ser^{423} was possibly phosphorylated due to only one serine and no threonine residue.

Reproduced with permission of the copyright owner. Further reproduction prohibited without permission.

Figure 3-18A

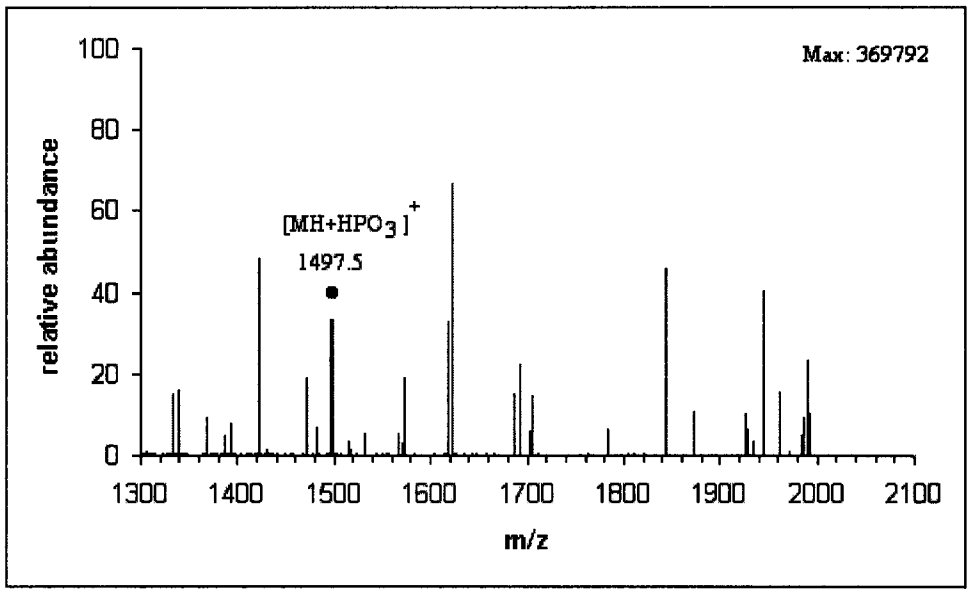

Reproduced with permission of the copyright owner. Further reproduction prohibited without permission.

Figure 3-19A and 19B. Analysis of unphosphorylated: EIEAIAGDGSEQAK

An observed unphosphorylated peptide (1417.0 Da) appeared in the deconvolution mass spectrum shown in Figure 3-19A and 19B.

Reproduced with permission of the copyright owner. Further reproduction prohibited without permission.

Figure 3-19A

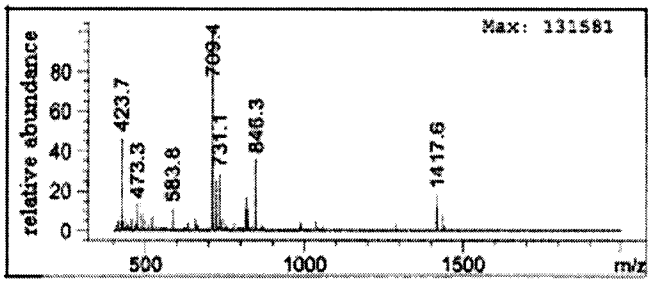

Figure 3-19B

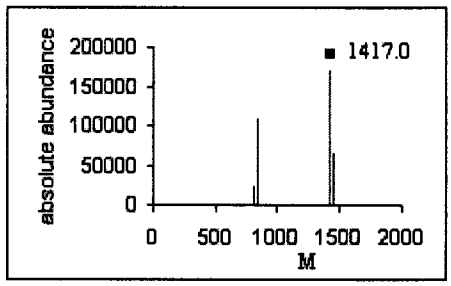

Reproduced with permission of the copyright owner. Further reproduction prohibited without permission.

Figure 3-20A. Analysis of phosphorylatrd SDDIDNWSR

The mass ion spectrum shown in Figure 3-20A resulted from total mixture peptides of IMAC run. The peptides ion at m/z 1187.3 present at 26.0 % of the most abundant peptide corresponds to the predicted phosphopeptide peptide with charge +1 at m/z 1187.5. The observed mass of 1186.3 Da matches the predicted mass (1186.5 Da) of the phosphorylated peptide 182-190 (SDDIDNWSR) with an increase of 80Da. This peptide contains two potentially phosphorylated sites, thus one phosphate can't be assigned to exact location.

Reproduced with permission of the copyright owner. Further reproduction prohibited without permission.

Figure 3-20A

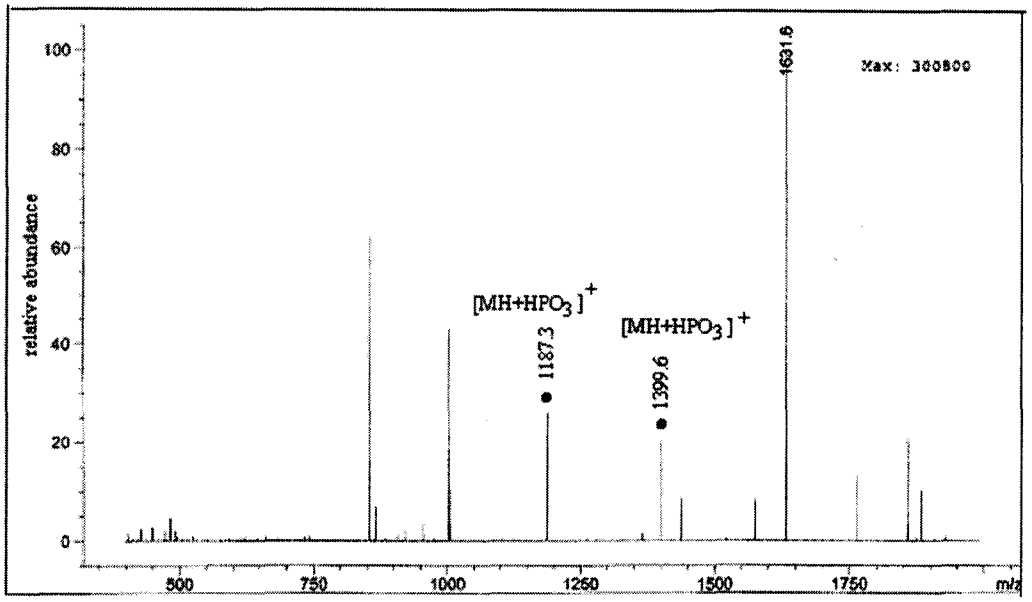

Reproduced with permission of the copyright owner. Further reproduction prohibited without permission.

Figure 3-21A. Analysis of phosphorylated peptide: SSR

The sample resulted from total mixture peptides of IMAC run. The ion mass spectrum in Figure 3-21A eluted from HPLC fraction. The peptide ion at m/z 313.3 in Figure 3-21A or expansion is in excellent agreement with a neutral loss of 98 Da from the predicated peptide ion 136-138 (SSR) containing one phosphorylated sites with +1 charge at m/z 331.2 (theoretical 349.2+80-98=331.2). The peptide was possibly phosphorylated at Ser^{138} and Ser^{139}.

Reproduced with permission of the copyright owner. Further reproduction prohibited without permission.

Figure 3-21A

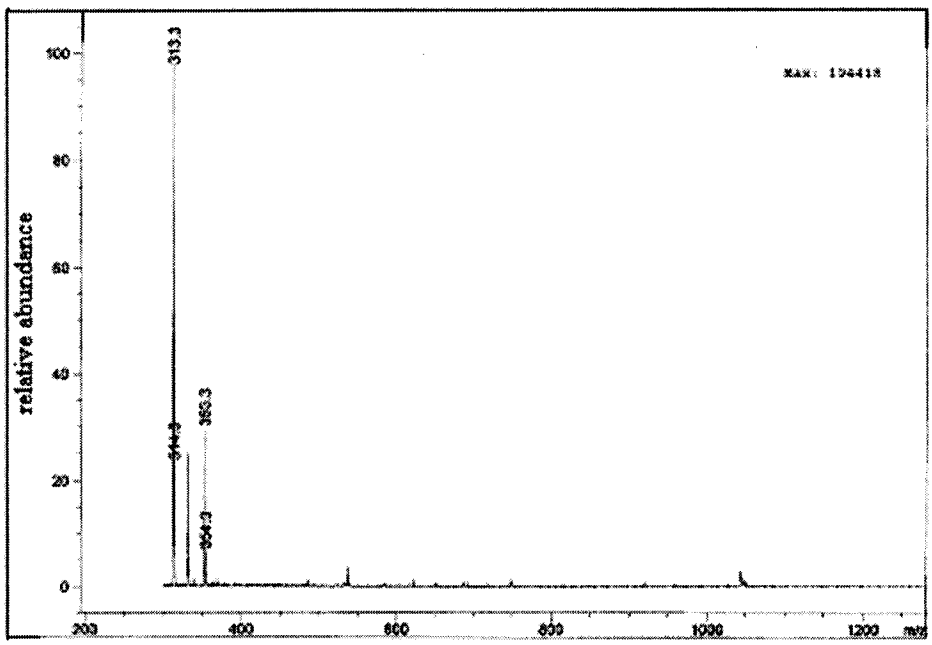

Reproduced with permission of the copyright owner. Further reproduction prohibited without permission.

Figure 3-21A- expanded

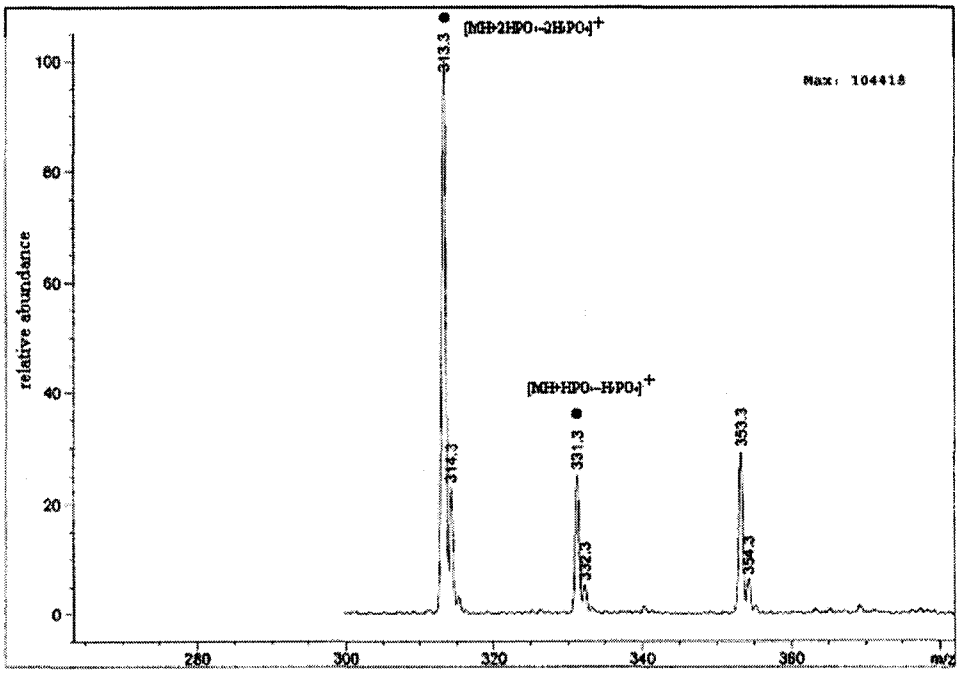

Reproduced with permission of the copyright owner. Further reproduction prohibited without permission.

Figure 3-22A and 22B. Analysis of phosphorylated peptide: ADESDNWGK or FGQRPSSGAGR

Negative-ion ESI mass spectrum was shown in Figure 3-22A and 22B. The observed mass of 1100.5 corresponds to two possible phosphorylated peptides. One is residues 148-156 (ADESDNWGK) with one phosphorylated site (theoretical 1020.4+80=1100.4). Another is residues 453-463 (FGQRPSSGAGR) with a neutral loss of 98Da (theoretical 1118.6-98=1100.6), so we could not identify which is the exact phosphorylated peptide based on the mass of 1100.5Da.

Reproduced with permission of the copyright owner. Further reproduction prohibited without permission.

Figure 3-22A

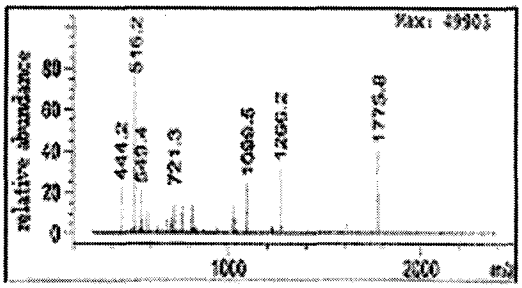

Figure 3-22B

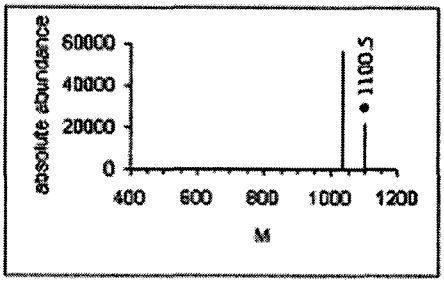

Reproduced with permission of the copyright owner. Further reproduction prohibited without permission.

REFERENCES

1. Pause, A., Methot, N., Svitkin, Y., Merrick, W.C., Sonenberg, N. (1994) *EMBO J* **13**, 1205-1215

2. Browning, K. S., Maia, D. M., Lax, S. R., and Ravel, J. M. (1987b) *J. Biol. Chem.* **262,** 538-541

3. Browning, K. S., Fletcher, L., Lax, S. R., and Ravel, J. M.(1989) *J. Biol. Chem.* **264,** 8491- 8494

4. Le, H., Browning, K. S., and Gallie, D. R. (1998) *J. Biol. Chem.* **273**, 20084- 20089.

5. Gallie, D. R., Le, H., Caldwell, C., Tanguay, R. L., Hoang, N. X., and Browning, K. S. (1997) *J. Biol. Chem.* **272**, 1046-1053

6. Duncan, R., and Hershey, J. W. B. (1984) *J. Biol. Chem* **259,** 11882-11889

7. Duncan, R., and Hershey, J. W. B. (1985) *J. Biol. Chem* **260,** 5493-5497

8. Bonneau, A. M., and Sonenberg, N. (1987) *J. Biol. Chem.* **262**, 11134-11139

9. Manzella, J. M., Rychlik, W., Rhoads, R. E., Hershey, J. W. B., and Blackshear, P. J. (1991) *J. Biol. Chem.* **266**, 2383-2389

10. Metz, A. M., Wong, K. C. H., Malmstrom, S. A., and Browning, K. S. (1999) *Biochemical and Biophysical Research Communications* **266**, 314- 321

11. Hunter, T. (2000) *Cell* **100**, 113-127

12. Graves, J. D., Krebs, E. D. (1999) *Pharmacol. Ther.* **82**, 111-121

13. Koch, C. A., Anderson, D., Moran, M. F., Ellis, C. and Pawson, T. (1991) *Science* **252**, 668-674

14. Hunter, T. (1994) *Semin. Cell Biol.* **5,** 367-376

Reproduced with permission of the copyright owner. Further reproduction prohibited without permission.

15. Dufner, A., Thomas, G. (1999) *Exp.Cell Res.* **253**, 100-109

16. Le, H., Browning, K. S., and. Gallie, D. R. (2000) *J. Biol. Chem.* **275**, 17452-17462

17. Mann, M., Ong, S. E., Grnborg, M., Steen, H., Jensen, O. N. and Pandey, A. (2002) *TRENDS in Biotechnology* Vol. 20 No.6, 261-267

18. Liao, P.C., Leykam, J., Andrews, P. C., Gage, D.A., Allison (1994) *J. Anal. Biochem.* **219**, 9-20

19. Andersson, L. and Porath, J. (1986) *Anal. Biochem.* **154**, 250-254

20. Li, S. and Dass, C. (1999) *Analytical Biochemistry* **270**, 9-14

21. Stensballe, A., Jensen, O. N., Olsen, J. V., Haselmann, K. F. and Zubarev, R. A. (2000) *Rapid Commun. Mass Spectrom.* **14,** 1793-1800

22. Vihinen, H. and Saarinen, J. (2000) J. Biol. Chem. 275, 27775-27783

23. Stensballe, A *et al.* (2001) Proteomics **1**, 207-222

24. Gaskell, Simon J., *J. Mass Spectrom.* (1997) **32**, 677-688

25. Kabarle, P., *J. Mass Spectrom.* (2000) **35**, 804-817

26. Iribane, J. V. and Thompson, B. A. (1976) *J. Chem. Phys.* **64** (6), 2287

27. Mann, M., Meng, C. K. and Fenn. J. B. (1989) *Anal. Chem.* **61**, 1702- 1708

28. Loo, J. A. (1997) *Mass Spectrometry Reviews*, **16**, 1-23

29. Loo, J. A., Udseth, H. R., Smith, R. D. (1989) Anal. Biochem. **179**, 404-412

30. Loo, J. A., Edmonds, C. G., Udseth, H. R., Smith, R. D. (1990) *Anal. Chem.* **62**, 693-698

31. Smith, R. D., Loo, J. A., Edmonds, C. G., Barinaga, C. J. and Udseth, H. R. (1990) *Anal. Chem.* **62**, 882-899

32. Covey, T. R.; Bonner, R. F.; Shushan, B. I.; Henion, J. (1988) *Rapid Commun. Mass*

Reproduced with permission of the copyright owner. Further reproduction prohibited without permission.

Spectrom. **2,** 249-256

33. Smith, R. D., Loo, J. A., Ogorzalek Loo, R. R., Busman, M., Udseth, H. R. (1991) *Mass Spectrom. Rev.* **10**, 359-451

34. Bouhallab, S., Oukhatar, N. A., Mollé, D., Henry, G., Maubois, J. L., Arhan, P. and Bougle, D. L. (1999) *Nutr. Biochem.* **10,** 723-727

35. Meng, C. K., Mann, M., Fenn, J. B. Z. (1988) *Phys. D.* **10,** 361-368

36. Mann, M., Meng, C. K., Fenn, J. B. (1989) *Anal. Chem.* **61,** 1702-1708

37. Yip, T. T., Hutchens, T. W. (1992) *FEBS Lett* **308,** 149-153

38. Bradshaw, R. A., Stewart, A. E. (1994*) Curr. Opin. Biotechnol.* **5,** 85-93

39. Craig, A. C., Hoeger, C. A., Miller, C. L., Coedken, T., River, J. E., Fischer, W. H. *Biol. Mass Spectrom.* (1994) **23**, 519-528

40. Zaluzec, E. J., Cage, D. A., Watson, J. T. (1995) *Protein Expression Purif.* **6**, 109-123

41. Biemann, K. and Scoble, H. A. (1987) *SCIENCE*, **237**, 992-998

42. Affolter, M., Watts. J. D., Krebs. D. L., Aebersold, R. (1994) Anal. Biochem. **223**, 74-81

43. Annan, R. S. and Carr, S. A. (1996) *Anal. Chem.* **68**, 3413-3421

44. Jonscher, K. R., Yates, J. R. *J. Biol. Chem.* (1997), **272,** 1735-1741

45. Stensballe, A., Jensen, O. N., Olsen, J. V., Haselmann, K. F. and Zubarev, R. A. (2000) *Rapid Commun. Mass Spectrum.* **14,** 1793-1800

46. Marin, O., Meggio, F., and Pinna, L. A. (1994) *Biochem. Biophys. Res. Commun.* **198,** 898- 905

47. Meggio, F., Marin, O., and Pinna, L. A. (1994) *Cell. Mol. Biol. Res.* **40**, 401-409

Reproduced with permission of the copyright owner. Further reproduction prohibited without permission.

48. Songyang, Z., Lu, K., Kwon, T. Y., Tsai, L., Filhol, O. Cochet, C., Brickey, D., R. T., Bartleson, C., graves, J. D., Demaggio, J. A., Hoekstra, F. M., Blenis, J., Hunter, T., and Cantley, L. (1996) *Mol. Biol. Cell* **16**, 6486-6493

49. Loo, J. A., Udseth, H. R., Smith, R. D. (1989) *Anal. Biochem.* **179**, 404-412

50. Loo, J. A., Edmonds, C. G., Udseth, H. R., Smith, R. D. (1990) *Anal. Chem.* **62**, 693-698

51. Barnes, S. " *Phosphorylation of proteins*", Feb 19th, 2002

52. Loo, J. A. (1997) *Mass Spectrometry Reviews* **16,** 1-23

Reproduced with permission of the copyright owner. Further reproduction prohibited without permission.